



LIBRARY Michigan State University

This is to certify that the thesis entitled

ALTERNATIVE MATERIAL FOR WORM GEARS USED IN WINDSHIELD WIPERS AND POWER WINDOWS

presented by

SARITA SRILAKSHMI MAHEEDHARA

has been accepted towards fulfillment of the requirements for the

MASTER OF SCIENCE

degree in

MECHANICAL ENGINEERING

Major Professor's Signature

6/5/2003

Date

MSU is an Affirmative Action/Equal Opportunity Institution

PLACE IN RETURN BOX to remove this checkout from your record. TO AVOID FINES return on or before date due. MAY BE RECALLED with earlier due date if requested.

DATE DUE	DATE DUE	DATE DUE
ARR3 0840	2 9 05	
<u> </u>		

6/01 c:/CIRC/DateDue.p65-p.15

ALTERNATIVE MATERIAL FOR WORM GEARS USED IN WINDSHIELD WIPERS AND POWER WINDOWS

Ву

Sarita Srilakshmi Maheedhara

A THESIS

Submitted to
Michigan State University
In partial fulfillment of the requirements
for the degree of

MASTER OF SCIENCE

Department of Mechanical Engineering

2003

ABSTRACT

ALTERNATIVE MATERIAL FOR WORM GEARS USED IN WINDSHIELD WIPERS AND POWER WINDOWS

By

Sarita Srilakshmi Maheedhara

Worm gears are used in windshield wipers and power windows of automobiles. The project proposed by Automation Tooling Systems, McAllen, Texas, was to eliminate several material problems resulting from the production of these worm shafts, such as production bottleneck and excessive scrap etc. from the original material, steel. A possible solution has been explored in this work by characterizing material properties of a promising candidate (glass reinforced acetal copolymer) that can replace steel in worm gears. Finite element analysis of the worm thread under service loads has been performed to make a preliminary estimate of the size of the new composite part. The results strengthen the possibility of the material replacement for the worm shaft without sacrificing part performance, whilst reducing part weight leading to improved fuel economy, noise reduction and manufacturing problems associated with the steel part.

This thesis is dedicated to my parents, Mr. Maheedhara Ramakrishna and Mrs
Maheedhara Annapurna, my sister Ms. Maheedhara Mrudula Archana and my
husband, Mr. Upadhyayula Sreeharsha

ACKNOWLEDGMENTS

I express my sincere appreciation to Dr.Farhang Pourboghrat and Dr.John Lloyd for all the patience, support and guidance they provided throughout my research. I would like to acknowledge the financial support from Automation Tooling Systems (ATS, McAllen, Texas), which helped me complete my research and graduate studies.

I would like to acknowledge Mr. Mike Rich, Dr. Tom Mase and Mr. Bob Jurek for their support in conducting the various experiments. I would also like to thank Mr. Steve Houle (ATS), Mr. Kenneth Rettmann (Visteon), Mr. Sujan E. Bin Wadud (TA Instruments), Mr. Frank Lach and Mr. Zan Smith (Ticona) for their generous resources and support.

I would like to thank my colleagues, Mr. Narasimhan, Mr. Ekbote and Mr. Ramcharan for their support and patience.

I am thankful to my parents and sister for their endless love and support.

Most importantly, I would like to thank my husband, Sreeharsha for his immense support, encouragement and patience.

TABLE OF CONTENTS

LIST OF TABLES v	⁄ii
LIST OF FIGURES	ix
LIST OF SYMBOLS	хi
CHAPTER 1 INTRODUCTION	1
CHAPTER 2 LITERATURE REVIEW	-
CHAPTER 3 3.1 EXPERIMENTAL WORK	14 15
3.2 GEOMETRY OF THE WORM	28
3.3 DETERMINATION OF THE FORCE COMPONENTS ACTING ON THE WORM	29
3.4 DETERMINATION OF VOLUME AND MASS OF MATERIAL	33
CHAPTER 4 FINITE ELEMENT ANALYSIS	35 36

4.2. MODEL DEFINITION	
CHAPTER 5 SUMMARY AND CONCLUSIONS	59
BIBLIOGRAPHY	60

LIST OF TABLES

Table 1.1. Mechanical Properties of Steel and Alternative Materials used for Worm Gear	3
Table 3.1.1. Temperatures set in various sections of the injection-molding machine	14
Table 3.1.2. Mechanical properties of GC25A at different temperatures	18
Table 3.1.3. Mechanical properties of M90 at different temperatures	18
Table 3.1.4. TTS results for glass reinforced composite	23
Table 3.1.5. Curve-fit for E(t) vs. time at various temperatures	24
Table 3.1.6. A (T), B (T) at varying temperatures	24
Table 3.1.7. A (T), B (T) from curve-fitting	25
Table 3.1.8 (a) E (T, t) from experiment and curve-fitting at 23°C	25
Table 3.1.8 E (T, t) from experiment and curve-fitting (b) at 40°C (c) at 60°C (d) at 80°C	26
Table 3.1.8 (e) E (T, t) from experiment and curve-fitting at 100°C	27
Table 3.2.1. Geometry of the worm and worm gear[37]	29
Table 3.3.1. Operational characteristics of the worm and the gear [Ref]	30
Table 4.1.1 (a) Calculated dimensions of the worm gear	40
Table 4.1.1 (b) Calculated dimensions of the worm gear (cont.)	41
Table 4.1.2 (a) Forces acting on the worm tooth	42
Table 4.1.2 (b) Forces acting on the worm tooth (cont.)	43
Table 4.2.1 No. of nodes and elements used in the FEA analysis	44
Table 4.2.2 Assumed material properties at initial time. to	45

Table 4.2.3 FEA results for GC25A at 23°C(a) at initial time, t ₀ (b) after 5 years	49
Table 4.2.3 (c) FEA results for GC25A at 23°C after 10 years	50
Table 4.2.4 (a) FEA results for GC25A at 105°C at initial time, t ₀	50
Table 4.2.4 FEA results for GC25A at 105°C (b) after 5 years (c) after 10	
years	51
Table 4.2.5 FEA results for GC25A at -40°C at initial time, t ₀	52
Table 4.2.6. FEA results for AISI 1144 Steel	52
Table 4.3.1. Volume of Composite material required	57

LIST OF FIGURES

Figure 1.1 Worm gear [ITW Spiroid, Chicago, IL]	4
Figure 1.2 Worm gears in garage door openers [5]	4
Figure 1.3 Wiper motor with worm gear [6]	5
Figure 3.1.1 (a) stress vs. strain graph of filled acetal	15
Figure 3.1.1 (b) stress vs. strain graph of unfilled acetal	16
Figure 3.1.2 GC25A after and before the uniaxial tensile test	17
Figure 3.1.3 (a) M90 before the test and at σ_{yield}	17
Figure 3.1.3 (b) M90 before the test and at σ_{ult}	17
Figure 3.1.4 Young's modulus (Mpa) vs. Temp. (°C)	19
Figure 3.1.5 Poisson's ratio vs. Temp. (°C)	19
Figure 3.1.6 Ultimate tensile stress (Mpa) vs. Temp. (°C)	20
Figure 3.1.7 Yield stress (Mpa) vs. Temp. (°C)	20
Figure 3.1.8 E (T) vs. time for GC25A at various temperatures	27
Figure 3.2.1 (a) Worm gear details [36]	28
Figure 3.2.1 (b) Worm Gear profile	28
Figure 3.3.1 Forces acting on the worm/worm gear pair	32
Figure 4.1.1 Line of action for worm-worm gear pair [37]	39
Figure 4.2.1 σ_{max} for Steel (axial pitch=1.92mm)—Left View	53
Figure 4.2.2 σ_{max} for Steel (axial pitch=1.92mm)—Right View	53
Figure 4.2.3 Equivalent plastic strain for Steel (axial pitch=1.92mm)	54

Figure 4.2.4 σ _{max} for GC25A@23C (axial pitch=1.92mm)	55	
Figure 4.2.5. Equivalent plastic strain for GC25A@23C (axial pitch=1.92mm)	55	
Figure 4.2.6 σ_{max} for GC25A@23C (axial pitch=2.25mm)—Left View	56	
Figure 4.2.7 σ _{max} for GC25A@23C (axial pitch=2.25mm)—Right View	56	

LIST OF SYMBOLS

 σ stress

 σ_y yield stress

 S_u , σ_{ult} ultimate tensile strength

 σ_k fatigue limit

 μ Poisson's ratio

 ε strain

 ε_p plastic strain

E Young's modulus

ρ density

D. P Diametral pitch

Chapter 1

INTRODUCTION

Gears are used for transmission of power and motion in many applications. A worm gear set consists of a shaft with helical threads and a wheel with teeth either parallel to the axis of rotation (spur gear) or at an angle to the axis (helical gear). Worm gears are used when the rotary motion has to be converted to linear motion and where large gear reduction ratios are desired. An interesting property of worm gears is that although they can rotate either way, there is only one allowable driving gear, the worm. That is, the worm can turn the gear; the gear cannot turn the worm, owing to the geometry of the worm. Worm gears are used in odometers, conveyor systems, Torsen (Torque Sensing) differentials [1], and most notably in business machines like printers/scanners/plotters where the crosshead travel is controlled by a worm gear. Worm gears are also used to drive the windshield wipers and power windows in automobiles.

Gears are made of metal, which makes parts that use gears heavy. Weight reduction has become a primary issue in many industries. Limited knowledge about the characteristics and behavior of plastics/composites, which are light in weight and are promising candidates for replacing metals, has led to extensive research in the plastics industry. The automotive industry, in particular, is exploring this 'switch-over' to plastics because of its many advantages.

Plastics are light in weight (which is important for fuel economy); they absorb shock and vibrations, and also reduce operating noise. They require little or no lubrication, and are corrosion resistant. Metals used in gears could be over-designed, and outlast the machinery they are a part of, while plastics, which are designed for the same purpose, would last for the appropriate service life.

Plastics allow design flexibility and are easily finished. They can be injection molded, thus eliminating the machining and finishing processes, which reduces production time and costs. The advantages of plastics offer promising future uses in many industries.

Plastics gears have some limitations. The load carrying capacity of plastics is low when compared to that of metals. From the Table (1.1), it is evident that plastics/composites are inferior in properties when compared to metals (steel in this case). Tensile strength of steel is 584.7Mpa, while Celcon M90 (at yield) is 66Mpa, which is 11% the strength of steel, whereas Celcon GC25A (at break) is120Mpa, which is 20% the strength of steel. Their behavior is largely dependent on working temperature, and they have a high coefficient of thermal expansion (COTE). Steel has a COTE of 16.6×10^{-6} /K, while that of Celcon M90 is 1.2×10^{-4} /K and Celcon GC25A= 0.3×10^{-4} /K.

Table (1.1) Mechanical Properties of Steel and Alternative Materials Used for Worm Gear

Material/ Property	Tensile strength (Mpa)	Coeff. Of thermal expansion (/ K)	Author
Steel	584.7	16.6 x 10 ⁻⁶	http://www.efunda.com/materials/alloys/ alloy_home/steels_properties.cfm
M90	66	1.2 x 10 ⁻⁴	Ticona
GC25A	120	0.3 x 10 ⁻⁴	Ticona

Although there are a few disadvantages in switching to plastic gears, the advantages outweigh the limitations. The following case study supports the choice of material made in this project: "A wear-resistant acetal copolymer allowed Whirlpool to produce a gear that lasts four times the normal machine life of its World Washer. The robust and long-lasting Splutch (Splined Clutch) Assembly can withstand 30Nm torque" [2]. Some companies (Maytag, Whirlpool) have recognized the benefits of switching to plastics, and claim that the plastic gears helped reduce part weight, as well as noise. They also claim that these gears are highly durable. [3]

Different types of non-metallic gears are currently being manufactured for various industrial purposes. 74% are spur gears, 15% helical, 5% worm, 4% bevel and the rest either epicyclic or internal gears. While the maximum diameter of a cut gear is 1m (reference circle diameter), injection molded gears saw a maximum of 200mm diameter. Approximately, 70% of the plastic gears manufactured, are injection molded. The most commonly used plastic

for gears is nylon (43%), followed by acetal (34%). Nearly 50% of them operate below a power of 10W and less than 10% at over 1kW. [4]

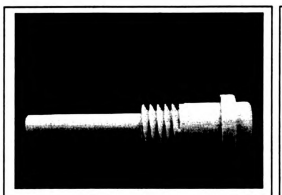


Figure 1.1 Worm gear [Courtesy of ITW Spiroid, Chicago, IL]



Figure 1.2 Worm gears in garage door openers [5]

The current project proposed by ATS McAllen, Texas, aims to eliminate several problems resulting from the production of worm shafts used in windshield wipers and power windows. These problems include production bottlenecks and excessive scrap. The objective of this project was to find an alternative material for the worm gear and wheel that can offer a service life of at least 10 years and also satisfy the design constraints (within the limited motor housing space). By finding suitable materials, the ultimate goals to minimize operating noise level, and operating vibration, maintain reliability, improve production output, and reduce manufacturing costs, will be met.

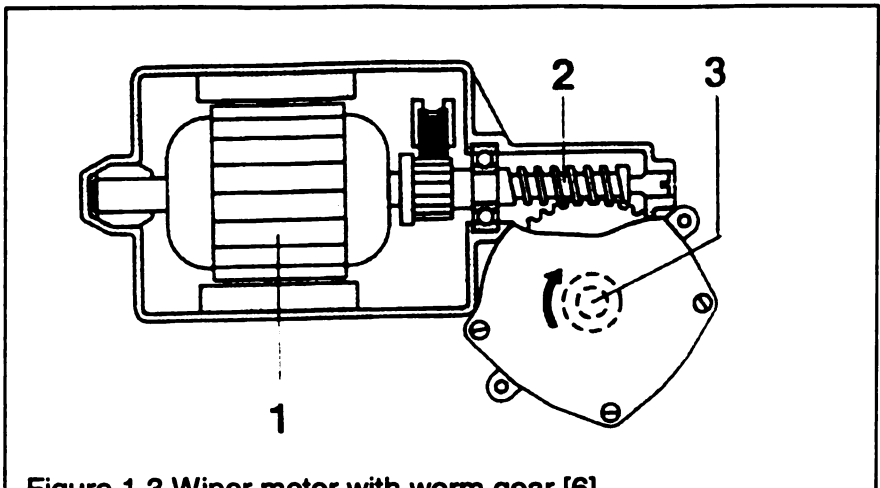


Figure 1.3 Wiper motor with worm gear [6]

1. Permanent-magnet DC motor, 2. Worm gear, 3. Shaft end

The first step involved identifying possible candidate materials, by comparing their mechanical properties as published by the suppliers. Two materials were selected and standard material tests, such as tensile test and creep test, were conducted to compare the material characteristics and to assess the suitability of these candidates for the specific application.

Finite element analysis was performed on the worm gear tooth, using the material properties obtained from the tests conducted. Thus a comparative study on the performance of the worm gear, using different materials, was done. The results are based on two criteria; one based on the properties obtained from experiments and the other was based on properties published [7]. The size of the gear made from composite should be 4.25 times the current size of the steel worm, to last for a year and 5 times the original size would last for 10 years when operating at a temperature of 105C, based on the first criterion, while those based on the latter one yields a size of 3.25

times the original size to last for a year and 3.5 times to last for 10 years operating at 105C.

Chapter 2

LITERATURE REVIEW

An effort to study the various effects and the trade-off paid by switching to plastic gears began as early as 1965. It has been cited in a European patent [8] that man-made materials are better than metals for worm gears, as their efficiency is relatively higher. Hooke, C.J et al (1993) [9] observed that the life of the gear depends on the tooth wear and not on fatigue at low loads. Several tests were conducted, and a conclusion reached that acetal has a sharp rise in wear, which was associated with the maximum surface temperature of the gear reaching the melting point of acetal, as the transmitted torque increased, thus limiting the use of acetal gears to low torque transmission. The efficiency of various combinations of plastic and steel gears with varying torques and running speeds was reproduced by Walton D et al (2002) [10]. The graphs showed that the efficiency of acetal /ABS - steel gear pair ranges from around 92% at low loads and increases up to 96% at the highest load and that the efficiency is speed-dependent and all the material combinations showed similar response to change in running speeds. It is seen that the acetal-steel pair is the better combination for any speed.

The efficiency of dry running plastic gear pairs is expected to be high at the start (near-static condition) and increase with increasing load (for some plastics) as the coefficient of friction decreases. Walton et al. [10] showed the efficiency of a pair of POM (acetal) gears over a range of loads and speeds under lubricated conditions. Performance of nylon6.6 (driver) - acetal pair (driven), which is a promising combination was discussed. It was demonstrated through experiments on a worm gear made of polymer composite, that the transmission efficiency increases when lubricated under O/W (Oil-in water) emulsions. This is due to self-lubrication of the material and also due to the formation of a water film [11].

It has been observed that the efficiency of the acetal gears is high and almost similar at low speeds, irrespective of the load. Also, efficiency is independent of the speed when it is more than 500rpm while it decreases by up to 10% when it ranges between 0 and 500rpm, and efficiency increases with increase in torque. Wear, which is a measure of loss of material, is relatively low in acetal gears running at a low torque of 7N-m. Acetal gears running at 1000rev/min and at low loads showed approximately linear wear and were nearly stable for sometime, and after a certain period, wear increased rapidly and failed due to plastic bending, which occurred due to material softening. If this material were overloaded, it would result in excessive wear and tooth breakage [12].

Assuming that the loss in efficiency is entirely due to friction, Walton D et al. derived friction coefficients for POM-POM gears for a range of loads and

speeds. An important implication made here is that the maximum contact stresses occur on the tooth flank surface when μ is greater than 0.3. A comparison of wear, wear rates and performance of acetal/acetal and nylon/nylon gears was made.

Vilmos Simon (1996) [13] performed stress analysis in worm gears. He demonstrated that considering multiple teeth for finite element analysis proves to be expensive in terms of memory size and computational time, while the difference in the displacements and stresses is relatively small. And hence, a single worm thread was considered for the finite element analysis for this project.

A conclusion was made in Simon 's work that stresses in the worm thread are strongly influenced by the number of worm threads, pitch diameter, tooth height and worm thread thickness factor while other worm design parameters have a moderate effect on the stresses. Hence, these parameters have to be borne in mind while designing the plastic worm. It was concluded that the performance of acetal is entirely dependent on wear and its life is limited to 500 hours at 1000 rev/min at low loads, and high wear rates could be explained as the result of surface temperature reaching the material melting point when transmission torque is increased.

The bending stress on the 10D.P. (Diametral Pitch) acetal gears should be limited to 2000psi, at a speed of 500 ft/min when running under dry conditions, for the gear to last for more than 10⁷ cycles. It has been observed

that a gear with fine pitch lasts longer than a coarse one as the former will heat up less. The gear life is affected by the operating speed, which directly affects the heat generation rate in a gear-pair. Gear life increases with speed when it is in the range of 600-1600ft/min. At higher speeds, heat generation increases and lubrication does not improve. [14]

John W. Kelly [15] proved that PK (aliphatic polyketones) has better properties in terms of creep rupture and impact resistance, when compared with POM, while POM (being a non-ductile polymer) is more creep-resistant. The gears used in windshield wipers and power windows experience stalled conditions, a stage where the rotation stops and the teeth in mesh experience instantaneous maximum load. Hence a study has to be made to measure the "accumulative creep strain" for acetal for the total stalled and cycled time. Approximate Notched Izod impact test (ASTM D-256) values for acetal at – 40°C and 23°C are 42.7 and 53.4 J/m respectively.

Paul Wyluda and Dan Wolf [16] conducted experiments and finite element analysis on acetal spur gears and came to a conclusion that the prediction of the behavior of acetal gears is a complex phenomenon and that it can be assumed linear elastic only for low loads and deformation. It was suggested that both experimentation and FEA should be conducted, and performing just one of the two would limit our understanding about the behavior of the plastic gear.

It has been ascertained that plastic gears can be used for power transmission and also the load carrying capacity of these gears can be increased by modifying the design (e.g. tooth profile modification, increasing the module to a value greater than 2) [17]. Though, it was initially suggested that nylon could be used for power transmission, later investigations proved that a phenomenon called creep occurred in the nylon gear, which influenced abrasion that occurs in these gears. [18]

Crippa G. and Davoli P., 1995 [19] concluded in their work that glass-reinforced composite should not be used to mate with steel gears, because, though they carry the advantage of improving the mechanical properties of the material, they cause wear (depending on their orientation), which is not acceptable in the industry. However, adding a lubricant could reduce this wear problem. Carbon fibers allow high torque transmission with acceptable wear. Further exploration is needed to compare the performance of carbon vs. glass-reinforced composites. It was also mentioned that plastic gears could see a torque of 20-45Nm for more than 10 million cycles, at a speed of 1500rpm and 3-7kW.

The material under consideration to replace steel worm was chosen as acetal (after an extensive search in the literature) as this material is considered to be the most popular of the structural plastics [20], [21]. It was also proved [20] that stress concentrations increase fatigue life, which is defined as the number of cycles of oscillation N before a specimen fractures at a given stress or strain [22].

Several analyses on plastic gears were performed using finite element methods [13, 16, 23]. An effort has been made in this paper to determine the mechanical properties of the plastic/ composite using the standard tests (ASTM D-638, DMA, DSC) and these properties were used in the finite element analysis of the worm thread, to determine the difference in the material behavior under similar loading. While in most works [13, 24], the load was assumed to act on the tip of the gear tooth and there is also evidence that several teeth carry load at all times [25]; for simplification of the problem, this paper looks at stresses when the load acts on the face of a single tooth.

A study of nylon gears for transmission of torque shows that they cannot be used without lubrication and also thermal conductivity is uneven throughout the gear, which results in the tooth breakage near the pitch point [26]. Though a similar behavior was seen in acetal, gears made of acetal seem to be a better choice for low torques, when wear has to be kept to a minimum [12]. Hooke C. J et al, 1996 [27] examined various materials, among which acetal and nylon existed and they concluded acetal gears were superior in performance and would last longer, provided the contact stress and maximum temperature do not exceed 50Mpa and 80° C respectively. If wear rate of $10^{-5} \mu m$ /cycle is acceptable, then they can see a temperature of 150° C. Significant crack formation was observed in case of nylon gears when they reached a temperature of 80° C.

Acetal gears can be successfully used to operate windshield wipers and power windows by modifying a few design parameters; for instance, the

uneven temperature distribution can be suppressed by using small modules, increasing the number of teeth as well as the face width, this also helps in increasing the load capacity. When the face width is increased, it should also be provided with ringed grooves to take care of the heat accumulated in the middle, due to the low thermal conductivity of the plastic [28]. An equation was developed to calculate the load capacity of the plastic gear using the bending stress at the pitch point (where most of the fractures occur) [24].

Chapter 3

3.1. Experimental Work

3.1.1. Injection-Molding

Celcon M90 and Celcon GC25A, which were kindly donated by Ticona (supplier), were chosen as the possible materials to replace steel in the worm gears. The former is a grade of acetal copolymer; while the latter is a grade of 25% glass filled acetal copolymer. The materials, which come in the form of pellets, were injection molded into tensile bars following the procedure mentioned in the data sheets. Table 3.1.1 shows the temperatures maintained in the different sections of the injection-molding machine. The injection speed was set to 12.7mm/sec (0.50in/sec) and 6.35mm/sec (0.25in/sec) for Celcon M90 and Celcon GC25A respectively. The screw was set to 40rpm speed and the fill pressure was set to a limit of 6.89Mpa (1000psi).

Table 3.1.1.Temperatures set in various sections of the injection-molding machine

	Set (°F)	Actual (°F)	
Nozzle	430	429	
Zone 1	400	400	
Zone 2	380	382	
Zone 3	340	340	

3.1.2 Uniaxiai tensile test

Universal Instron test machine was used to conduct uniaxial tensile test on Celcon M90 and Celcon GC25A to determine the material behavior at different temperature levels. The temperatures at which the specimens were tested are 150C, 23C, and -40C. Longitudinal and transverse extensometers were used when applicable. Maximum travel for the longitudinal gage was 10% (2.54mm extension) and for transverse gage was 2% (0.508mm). The crosshead speed was maintained at 1mm/min. Five specimens for the filled material and five to ten for the unfilled were tested at each temperature. The filled bars behaved predictably (Fig. 3.1.1 (a)), and a typical stress-strain curve was obtained, while the unfilled bars did not break (Fig. 3.1.1(b)).

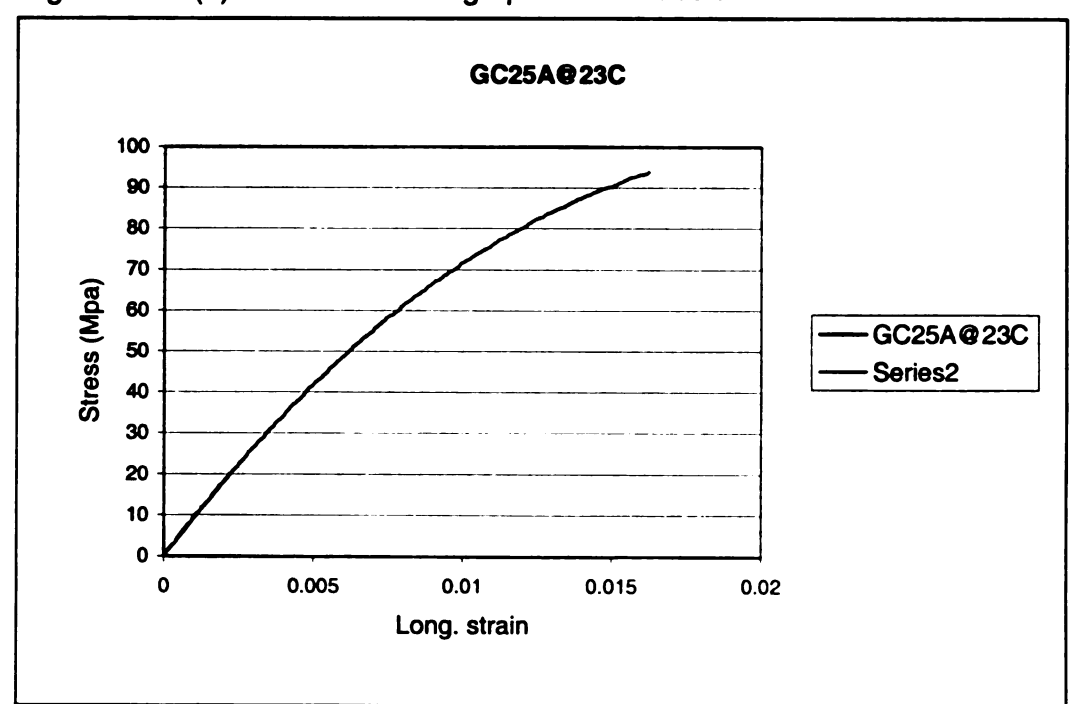
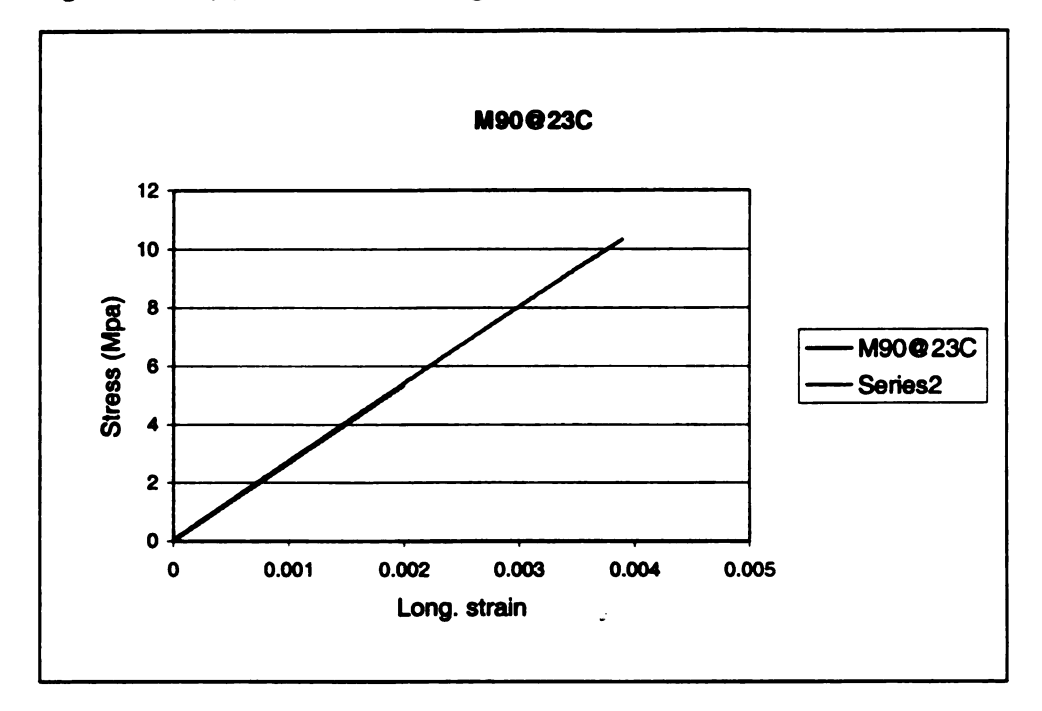


Figure 3.1.1 (a) stress vs. strain graph of filled acetal





The test could not be conducted up to failure using the extensometers on the unfilled specimens. If the stress-strain curve was linear the same test bar was used to determine the ultimate load and when this curve turned non-linear, a different specimen was used to determine the peak load. Since the unfilled specimen did not yield, nor break, the ultimate load was assumed at the point on the curve where the peak load was constant. The specimens were kept at room temperature and 50% relative humidity. When tested at temperatures other than the room temperature, the specimens and the grips were quenched to that temperature in an Applied Test Systems Programmable oven for at least 60 minutes to allow the test specimens as well as the grips to have a uniform temperature. The tests show that the material behavior largely depends on the temperature.



Figure 3.1.2. GC25A after and before the unixial tensile test



Figure 3.1.3. (a) M90 before the test and at $\sigma_{\text{yield}},$



(b) M90 before the test and at σ_{ult}

Table 3.1.2 Mechanical properties of GC25A at different temperatures

Temp(C)	E (Mpa)	μ	Ult. tensile stress(Mpa)	Yield stress (Mpa)
-40	10257.372	0.401	138.345	20.514
23	8816.213	0.472	94.926	17.632
150	4854.369	0.542	47.145	9.708

Table 3.1.3 Mechanical properties of M90 at different temperatures

Temp(C)	E (Mpa)	μ	Ult. tensile stress (Mpa)	Yield stress (Mpa)
-40	3588.22	0.374	83.001	7.176
23	2857.67	0.427	54.387	5.715
150	952.78	0.424	20.925	1.905

From Tables 3.1.2 and 3.1.3, it is seen that the material properties change with temperature. Tensile strength of the material has been defined as the stress needed to break the sample [29]. While the tensile strength and young's modulus of both grades of Celcon decreased with increasing temperature, Poisson's ratio increased with an increase in temperature. Then, the fatigue limit, σ_k , which is generally assumed as 30-40% of the tensile strength is also influenced by the temperature [30].

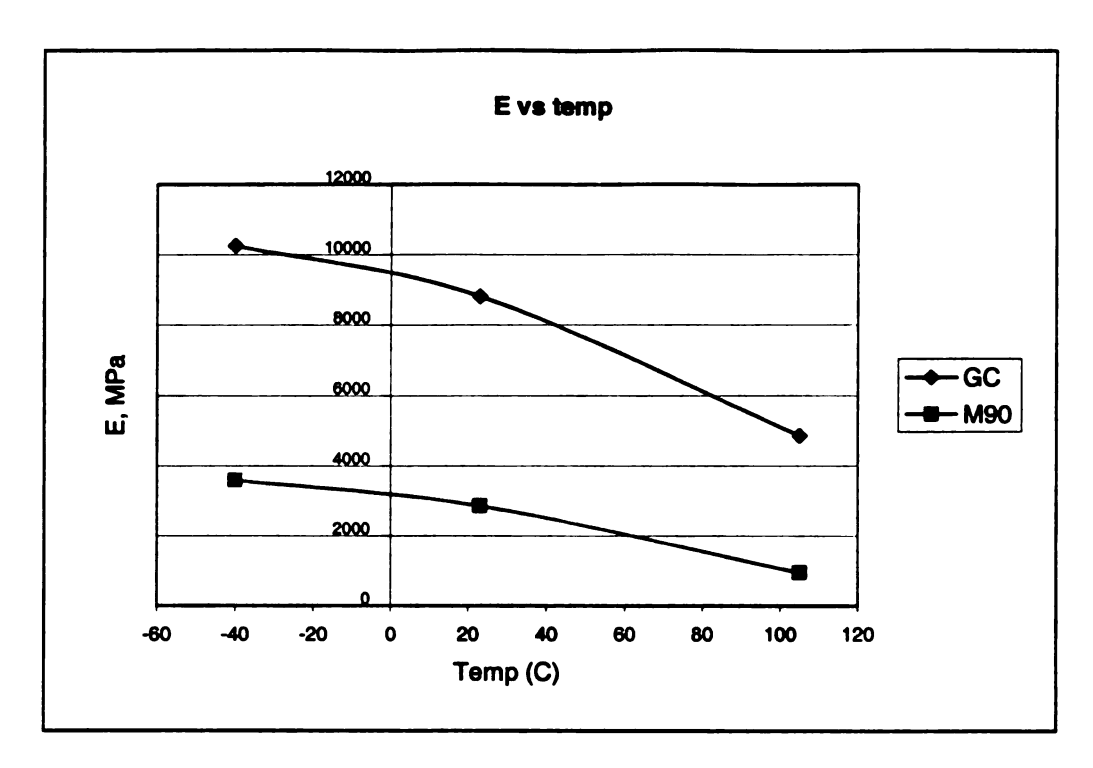


Figure 3.1.4 Young's Modulus (Mpa) vs. Temp. (°C)

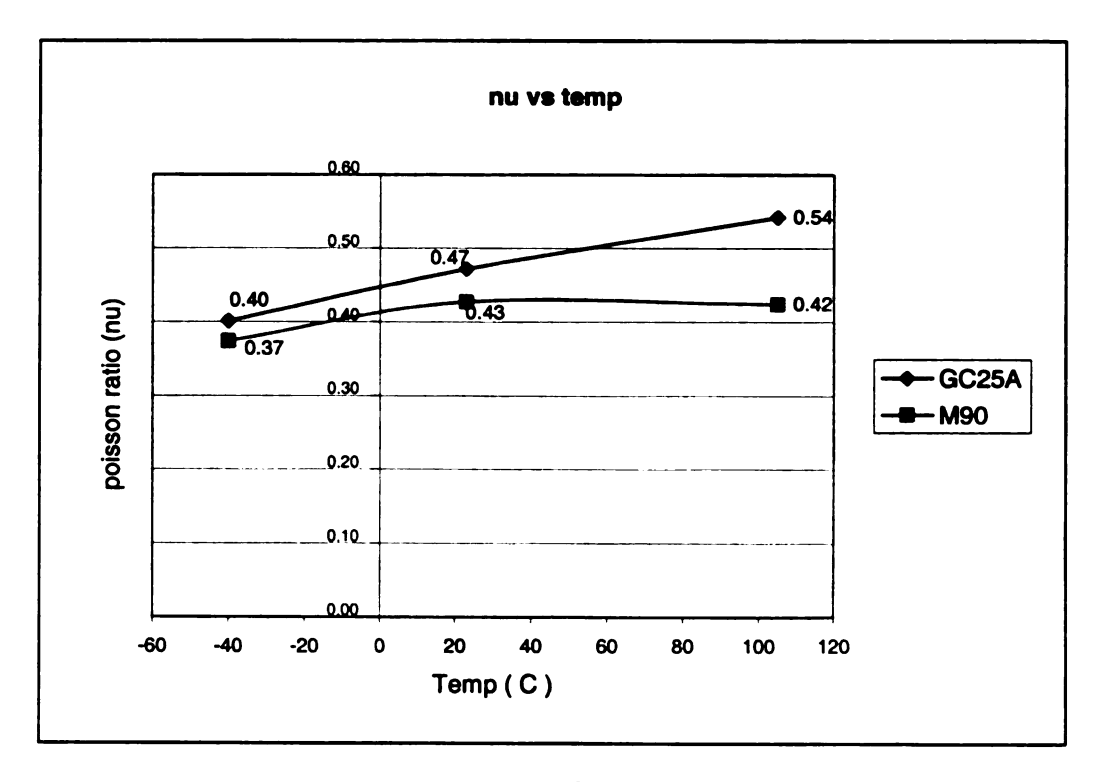


Figure 3.1.5 Poisson's ratio vs. Temp. (°C)

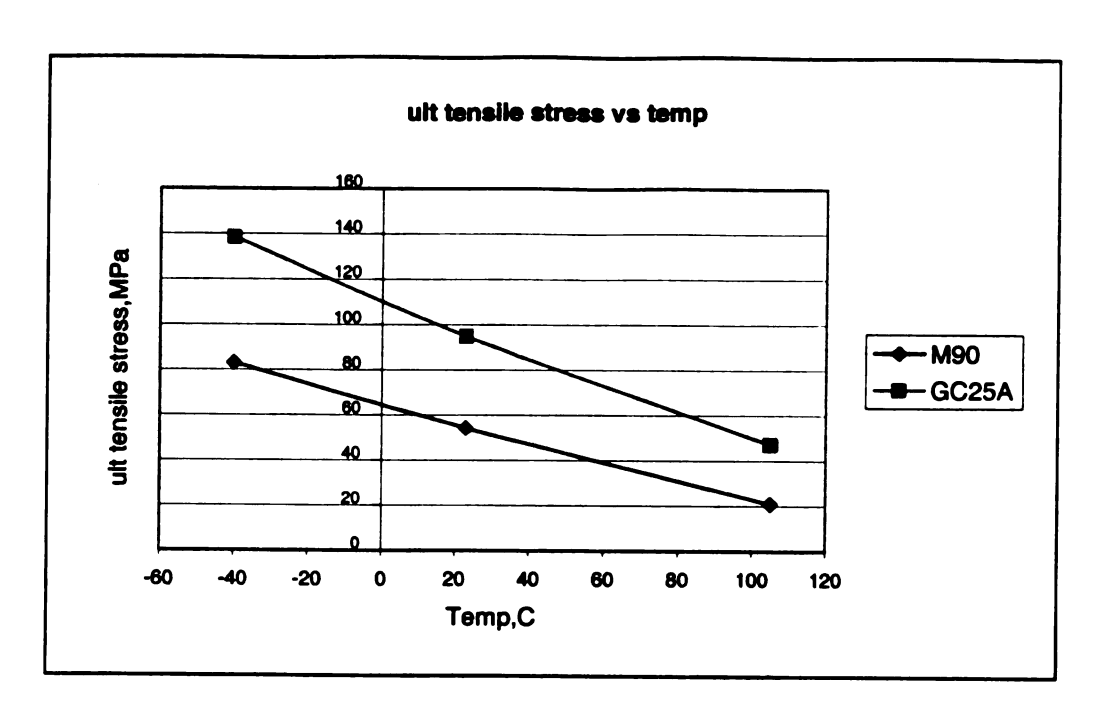


Figure 3.1.6 Ultimate tensile stress (Mpa) vs. Temp. (°C)

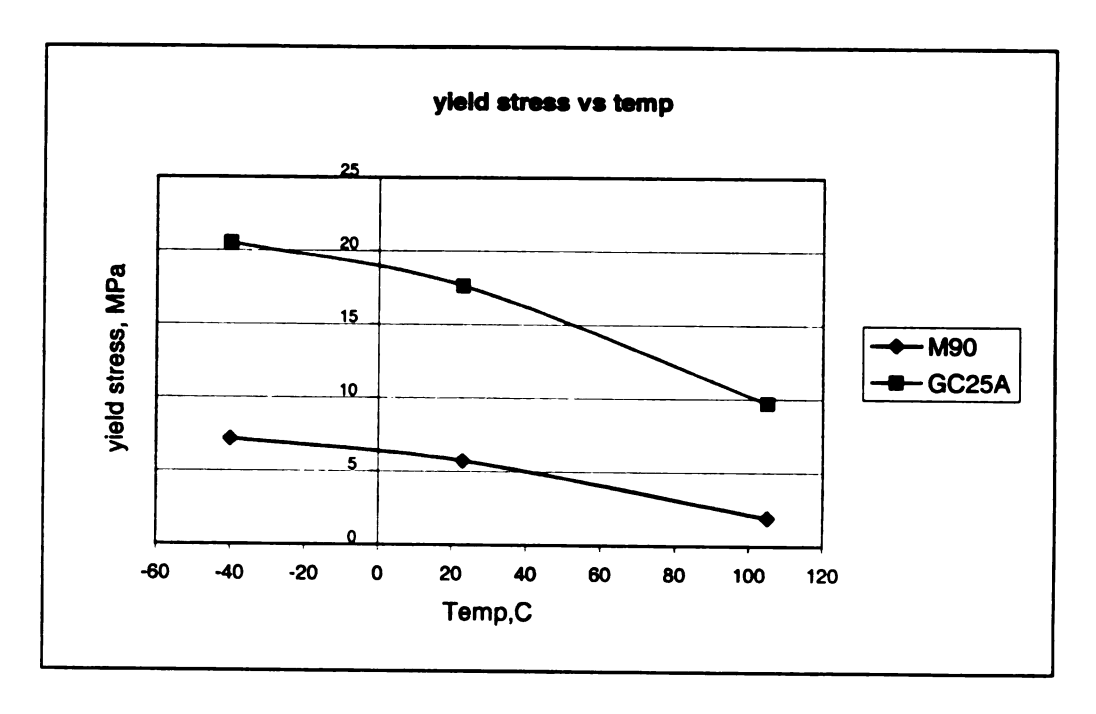


Figure 3.1.7 Yield stress (Mpa) vs. Temp. (°C)

Though the neat plastic Celcon M90 did not show a yield point during the uniaxial tensile test, for the purpose of running a non-linear analysis, yield was assumed at the same point where the glass-reinforced plastic yielded. Using Considere criterion $[\frac{d\sigma}{d\varepsilon} = \sigma]$ and power-law hardening equation $[\sigma = k\varepsilon^n]$, we obtain the relation $n = \varepsilon$ to be the limiting strain at which uniform elongation ends and necking begins under the uniaxial deformation. Assuming that $\sigma = \sigma_y$ at $\varepsilon = 0.002$, n can be solved, iteratively, using the

formula:
$$n = \frac{\ln(\sigma_y) - \ln(S_u)}{\ln(0.002) + \ln(e) - \ln(n)}.$$

It has been demonstrated [31] that the values of k and n, thus calculated give more accurate results and hence values obtained from the above calculations have been used in the non-linear finite element analysis. For different values of ε_p assumed, corresponding stress values were obtained using the power-law relation.

3.1.3 DMA Creep test

Though some experts were skeptical about using Dynamic Mechanical Analysis (DMA) for creep prediction of composites, it has been stated [32] that the time temperature superposition is applicable to fiber-reinforced plastics, though only for short-term creep.

The viscoelastic nature of polymers causes their deformation to depend on time as well as temperature. The characteristic of viscoelasticity is that the elastic modulus of the material decreases over a period of time for a

constant load, due to molecular rearrangement within the polymer. Time-temperature superposition principle states that this behavior of molecular rearrangement at a particular temperature over a long period of time can be conveniently predicted by conducting DMA such as creep, stress relaxation, etc at elevated temperatures for a shorter period of time [33].

Stress relaxation experiment was conducted to determine the longterm properties of the materials. This procedure involves applying stress on the specimen to maintain constant strain (of value 1.0) at different temperatures, and this stress is measured as a function of time. The stress relaxation modulus is obtained by dividing time dependent stress by constant strain (TA Instruments Rheology Advantage Manual, [34]. Once this data is recorded, using time-temperature superposition principle (TTS), we obtain the corresponding modulus (E (t)) value at the reference temperature, which is a function of time. A specimen of rectangular cross-section of dimensions 5 x 12.4 x 1.23 (mm x mm x mm) was used for conducting the stress relaxation experiment. It has been demonstrated that creep experiments exhibit excellent repeatability (2.3%) [35]. Due to lack of experimental resources at the appropriate time, the tests were conducted only on single specimens of each material, at the TA Instruments head office, Delaware. The results obtained from this experiment have been tabulated with select data points as in Table 3.4 for glass-reinforced acetal.

Table 3.1.4 TTS results for glass reinforced composite

Temp. = 23C			Temp. = 40C		
	time, yr	E (T) Mpa		time, yr	E (T) Mpa
	1	4690		1	3779
	2.5	4462		2.5	3596
	5	4304		5	3438
	7.5	4207		7.5	3369
	10	4123		10	3394
Temp. = 60C			Temp. = 80C		
	time, yr	E (T) Mpa		time, yr	E (T) Mpa
	1	2502		1	1598
	2.5	2391		2.5	1501
	5	2290		5	1437
	7.5	2239		7.5	1404
	10	2181		10	1386
Temp. = 100C					
	time, yr	E (T) Mpa			
	1	1142			

Data about the material behavior of the composite at 100C after 10 years could not be obtained with this experiment; hence it was done by extrapolation with the existing values. A graph was drawn for E (t) vs. time over a period of 10 years at temperatures where data was recorded, and a curve-fit to these graphs resulted in constants A (T) and B (T) (Table 3.1.5). The general form of the curve-fit to each of the plots is of the form:

E(T,t) = A(T) Ln(t) + B(T). The variation of these constants with temperature (Table 3.1.6) was plotted and fitting a polynomial to these curves gave a set of equations for A(T) and B(T), which were then used to calculate the unknown value of E at 100C. Now, plugging these values of constants into the general form of the curve-fit yields E(T, t), i.e., E is obtained as a function of time and

temperature. Assuming a constant error in the value of E (T, t) between the experimental and the curve-fit at 100C, values were extrapolated for the experimental set-up (which was then incorporated in the finite element model).

The procedure used to predict the material property of the composite operating at 100C is depicted below:

Table 3.1.5 Curve-fit for E (t) vs. time at various temperatures

Temp. C	Curve Fit for E (t) vs. time graph
23	y = -247.26Ln(x) + 4689.3
40	y = -213.2Ln(x) + 3812.9
60	y = -155.77Ln(x) + 2540.6
80	y = -97.476Ln(x) + 1603.9
100	y = -102.53Ln(x) + 1090.6

Table 3.1.6 A (T), B (T) at varying temperatures

Temp. C	A (T)	B (T)
23	-247.26	4689.3
40	-213.2	3812.9
60	-155.77	2540.6
80	-97.476	1603.9
100	-102.53	1090.6

The polynomials obtained for A (T) and B (T) are:-

A (T): y = -0.0009x3 + 0.148x2 - 4.7729x - 204.04

B (T): y = 0.007x3 - 1.0273x2 - 10.647x + 5401.2

Table 3.1.7 A (T), B (T) from curve-fitting

Temp. C	A (T)	B (T)
23	-246.475	4698.046
40	-215.756	3779.64
60	-152.014	2576.1
80	-99.472	1558.72
100	-101.33	1063.5

Table 3.1.8 E (T, t) from experiment and curve-fitting at (a) 23C (b) 40C (c) 60C (d) 80C (e) 100C

Table 3.1.8 (a)

Temp., C				
23	time, yr	E(T)	experimental	error%
	1	4698.0463	4690	-0.17
	2.5	4472.204	4462	-0.23
	5	4301.360	4304	0.06
	7.5	4201.423	4207	0.13
	10	4130.517	4123	-0.18
	Avg.			-0.08

Table 3.1.8 (b)

Temp., C				
40	time, yr	E(T)	experimental	error%
	1	3779.640	3779	-0.02
	2.5	3581.945	3596	0.39
	5	3432.394	3438	0.16
	7.5	3344.913	3369	0.71
	10	3282.843	3394	3.28
	Avg.			0.91

Table 3.1.8 (c)

Temp., C				
60	time, yr	E(T)	experimental	error%
	1	2576.1	2502	-2.96
	2.5	2436.811	2391	-1.92
	5	2331.443	2290	-1.81
	7.5	2269.807	2239	-1.38
	10	2226.075	2181	-2.07
	Avg.			-2.03

Table 3.1.8 (d)

Temp., C				
80	time, yr	E(T)	experimental	error%
	1	1558.720	1598	2.46
	2.5	1467.575	1501	2.23
	5	1398.626	1437	2.67
	7.5	1358.294	1404	3.26
	10	1329.677	1386	4.06
	avg			2.93

Table 3.1.8 (e)

Temp., C				
100	time, yr	E(T)	experimental	error%
	1	1063.5	1142	6.87
	2.5	970.652	1042.299	6.87
	5	900.416	966.878	6.87
	7.5	859.330	922.759	6.87
	10	830.179	891.457	6.87

The numbers in experimental column for Temp.=100°C for time 2.5 to 10yrs are estimated

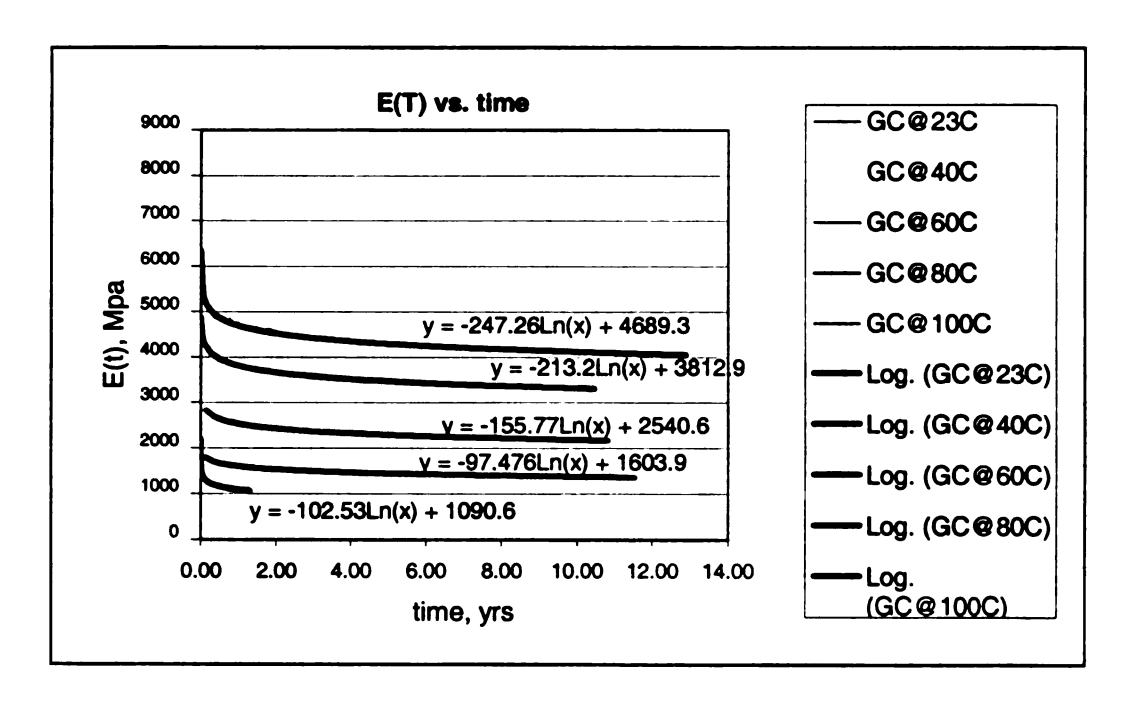
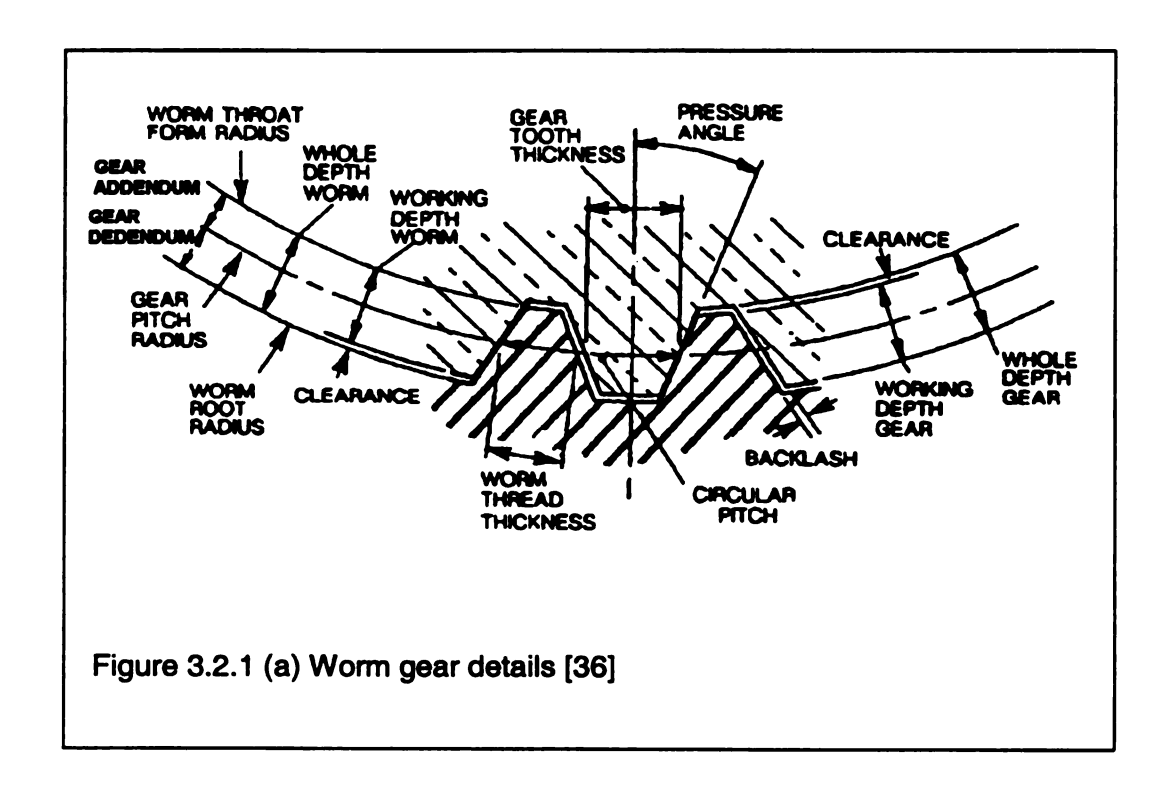


Figure 3.1.8. E (T) vs. time for GC25A at various temperatures

3.2 GEOMETRY OF THE WORM

The finite element model of the worm is based on the design data provided by Visteon Wiper/Washer Engineering. The worm dimensions are as stated in Table 3.5.



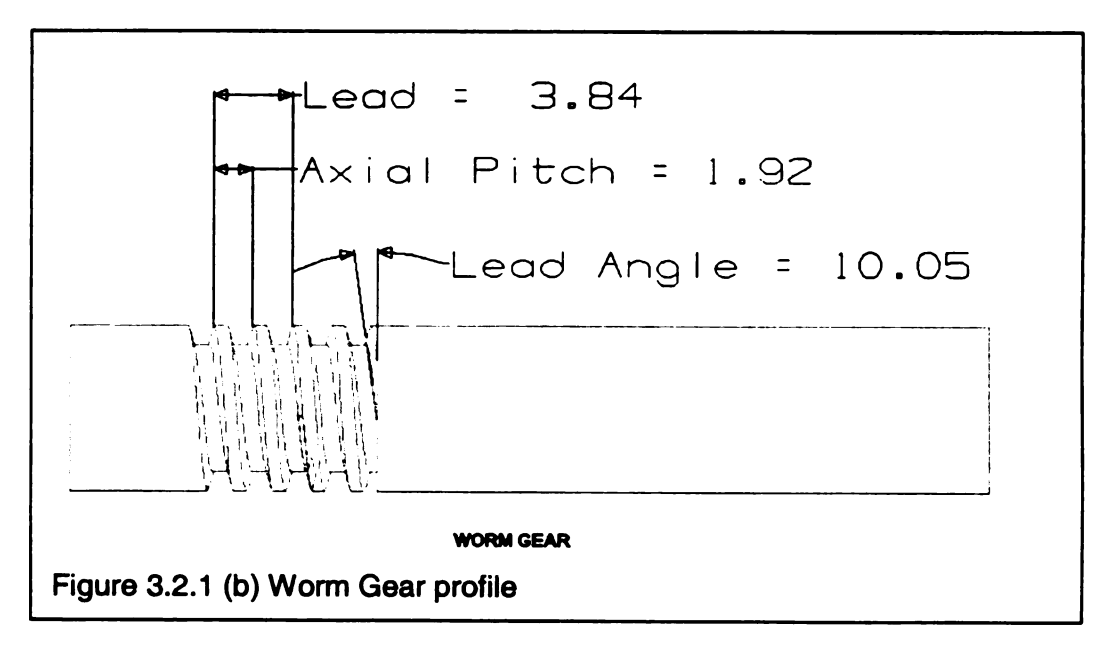


Table 3.2.1 Geometry of the worm and worm gear [37]

	Worm gear	Worm
Major diameter	62.86±0.076	8.465±0.032
Root diameter	59.56±0.076	5.00±0.05
Tooth form	Involute	Involute
Normal module	0.6025	0.6025
Axial lead	1084.2	3.845
Circular tooth thickness	1.156±0.03	0.734±0.025
Pitch diameter	61.19	6.88
Lead angle, λ	_	10.0540
Normal circular pitch	1.89	1.89
Axial pitch	-	1.92
Normal pressure angle, Φ _n	14.50	14.50

3.3 DETERMINATION OF THE FORCE COMPONENTS ACTING ON THE WORM

Fig.3.7 illustrates the force components (tangential, radial and axial) that act on the worm and the worm gear for a windshield wiper. As the exact mechanism for a windshield wiper is not clear, the forces have been assumed to be operating on the power window for the analysis. The FE model has been simplified by neglecting the friction force components. The force components are derived using the following formulae [38]:

Load Data

Maximum Sliding Velocity, V_s = 85.2cm/sec = 167.72ft/min

Coefficient of friction for V_8 =167.72 ft/min., f =0.05 [39] (this is approximately equal to the value given in the design data, f = 0.046).

Rotational speed and torque characteristics of the worm and the gear, considered for the force analysis, are given in Table 3.6.

Table 3.3.1 Operational characteristics of the worm and the gear.

	(Driver) Worm	(Driven) Worm gear		
Rotational speed (rpm)	1950.0	39.0		
Torque (N-m)	0.8643	34.0		

Number of teeth on the worm gear, $N_g = 100$

Number of teeth on the worm, $N_w = 2$ (the number of teeth on the worm is equal to the number of starts)

Stall force (Tangential) on Worm Gear:

$$F_{gt} = \frac{2T_g}{d_g} = \frac{2 \times 34.0}{0.06112} = 1112.57N$$
 (Tangential force on the worm gear = axial

force on the worm, $F_{gt} = F_{wa}$)

But, this force is the total force acting on two teeth (as the number of starts is two, hence two teeth mesh at any point of time with two teeth of the mating gear, thus the load is distributed between two teeth).

$$\therefore$$
 Axial force per worm tooth, $F_{gt} = F_{wa} = \frac{1112.57N}{2} = 556.28N$

Worm Tangential force:

$$F_{wt} = \frac{2T_w}{d_w} = \frac{2 \times 0.8643}{6.88 \times 10^{-3}} = 251.25N$$

(Axial force on the worm gear = tangential force on the worm, $F_{ga} = F_{wt}$)

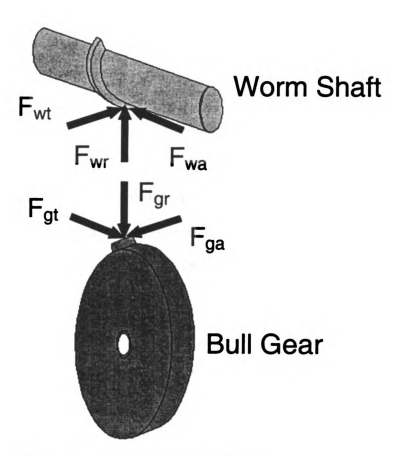
$$\therefore$$
 Tangential force per worm tooth, $F_{ga} = F_{wt} = \frac{251.25N}{2} = 125.63N$

Radial force:

$$F_{gr} = \frac{F_{gt} \cdot \tan \phi}{\cos \lambda} = \frac{1112.56 \times \tan(14.5)}{\cos(10.05)} = 292.21N$$

(Radial force on the worm gear = Radial force on the worm, $F_{gr} = F_{wr}$)

$$\therefore$$
 Radial force per worm tooth, $F_{gr} = F_{wr} = \frac{292.21N}{2} = 146.1N$



Force Components

$$F_{gt} = F_{wa} = 1112.56 \text{ N}$$

$$F_{gr} = F_{wr} = 292.2 \text{ N}$$

$$F_{qa} = F_{wt} = 251.25 \text{ N}$$

Fig.3.3.1 Forces acting on the worm/worm gear pair

3.4 DETERMINATION OF VOLUME AND MASS OF MATERIAL

The total volume of material required to produce a worm gear from plastic/composite can be determined by calculating the volume of the cylinder (cylinder formed from inner radius) and the volume of the helical thread. For the case of steel, the material is machined to make the thread and hence the total volume of material required would be equal to the volume of the outer cylinder. The volume of the helical thread can be determined by considering its cross-section as a trapezoid. The length of the helix can be determined from the axial pitch and inner radius [40]. The relations can be framed as below:

Length of threaded worm using steel = 35 mm

Total length of the steel shaft = 181.2 mm

Diameter (pitch) = 6.88 mm

Major Diameter = 8.465 mm

Minor Diameter = 5.0 mm

No. of threads $=N_w \times (length of threaded worm/axial pitch)$

For a double threaded worm, $N_w = 2$

Density of steel, $\rho_s = 7.87 \text{ gm/cm}^3$

Density of GC25A, $\rho_{GC} = 1.58 \text{ gm/cm}^3$

Price of steel per in³ = \$ 0.471 = 0.00287cents/mm³

Price of GC25A per $in^3 = $0.053 = 0.000323cents/mm^3$

Volume of the steel material required =
$$\left[(shaft - length) \times \pi r_o^2 \right]$$

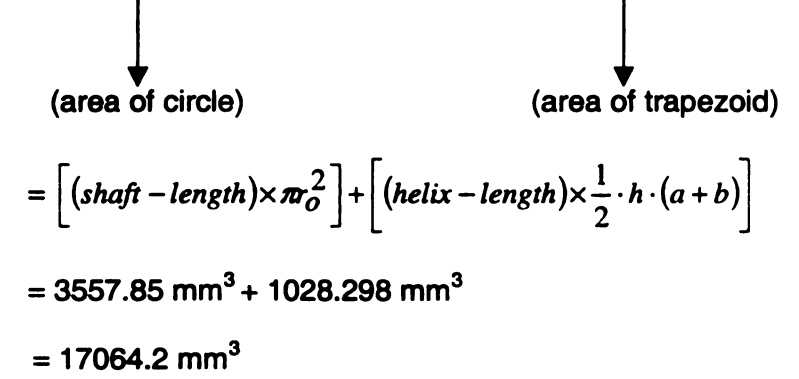
= 10197.69 mm³

 \therefore Mass of steel required, $M_s = \rho_s \times 10197.69 \text{ mm}^3 = 0.0803 \text{Kg} = 80.26 \text{gm}$

Price of one steel cylinder = 29.26 cents

Volume of plastic material used = volume of solid shaft + volume of helix

= (shaft length x c.s area of shaft) + (length of helix x c.s area of helical thread)



where, inner radius of the shaft = r_i = 5.0 mm

tooth height = h = 1.32 mm

parallel sides of the trapezoid, a = 0.634 mm

b = 1.34 mm

Chapter 4

FINITE ELEMENT ANALYSIS

A finite element model of a shaft with a single worm thread was developed using Unigraphics®. Hypermesh® was used to develop the mesh and to assign the boundary conditions and material properties and solver used was ABAQUS implicit code, V6.3 [41]. Tetra 4 elements were used for analyzing the material response. Though it is suggested to avoid tetra elements due to their inefficiency to provide converging solutions [41], it is a common practice to use them in most industrial applications dealing with complex geometries; therefore the tetra 4 has been used for this analysis. Both ends of the shaft were fixed and the force components calculated in Chapter 3 were applied to a portion of the face (where the arc length was approximately equal to the face width of the gear, 4.6mm) Properties of three different materials, steel, Celcon M90 and Celcon GC25A shown in Table 4.2.2 were applied to the model. Material properties for the plastic and composite were obtained from experiments conducted at different temperatures, -40C, 23C, and 105C.

For the purpose of simplicity, following assumptions are made in the finite element analysis: (i) materials are within the linear elastic range (ii) materials are isotropic (iii) loads applied are static in nature. The composite was also assumed as an isotropic material due to various reasons, foremost

being, for simplicity. Fiber orientation and distribution in an injection molded component largely depends on the component geometry, molding conditions, such as gating, pressure, temperature and holding time, matrix material, polymer melt viscosity, characteristics of fiber, such as density, aspect ratio and volume fraction [42]. By assuming that all these factors were chosen carefully so that the fibers were randomly oriented, and hence an assumption that it is isotropic is justified.

4.1. REDESIGN OF THE WORM WITH PLASTIC

The initial analysis was performed on the model with original worm dimensions. As expected, the results went into the plastic region. Using the following set of relations, (which slightly deviate from the worm design standards); the dimensions of the model were gradually increased and depending on the results, were modified until an optimum design was reached which was well within elastic limits:

Relations used in designing a worm1:

Pressure angle, $\Phi_n = 14.5$

Axial pitch, $p_x = 1.92$

No. of threads on the worm, $N_w = 2$

Lead angle, $\lambda = 10.05^{\circ}$

Helix angle, $\beta = (90 - \lambda) = (90 - 10.05) = 79.95^{\circ}$

Lead, $L = N_w \cdot p_x$

Normal circular pitch, $p_n = p_x \cos \lambda$

Diametral pitch, $P_d = \pi / p_n = 1.66$

¹ All units in mm

Circular pitch, $P_c = p_r/\cos \beta = 10.81$

Pitch diameter, $d_w = L / \pi \tan \lambda$

Addendum, $a = (1.0/ P_d) = (1.0/1.66) = 0.602$

(these relations are meant for a spur gear)

Dedendum, $b = (1.25/P_d) = (1.25/1.66) = 0.753$

Whole depth, $h_t = 0.6866 p_x = 0.6866*1.92 = 1.318$

Working depth, $h_k = 0.6366^* p_n$

O.D,
$$d_0 = d_w + 2a = 6.882 + 2(0.602) = 8.08(~8.465)$$

I.D,
$$d_i = d_0 - 2h_1 = 8.08 - 2(1.318) = 5.36(\sim 5.0)$$

Face width of gear, $F_g = 0.67 d_w$

Tooth thickness, $t_w = 0.5 p_x \cdot \cos \lambda$

Dimensions required for the design:

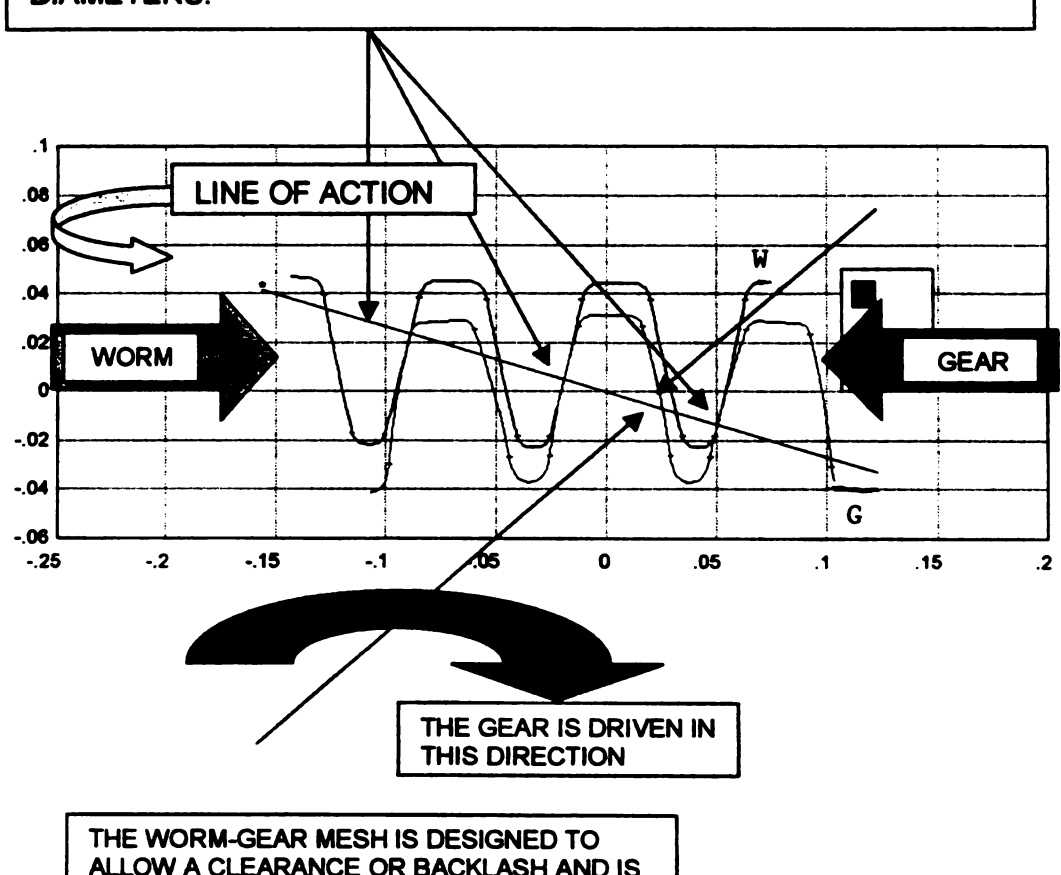
- 1) Axial pitch, p_x
- 2) Major diameter, O. D.
- 3) Root diameter, I.D.
- 4) Angle between 2 teeth, $2\Phi_n$ [this is constant]

Tables 4.1.1 (a) and (b) describe the gear dimensions for different values of axial pitch. Table 4.1.2 (a) and (b) show the different force components acting on the gear tooth based on the force analysis described in Chapter 3.3. The desired output torque being constant, the increase in the gear dimensions results in smaller forces acting on it. Since, the load acts over an area, it has to be applied as DLOAD, which is similar to pressure. The area over which the force components act (area of contact, Figure 4.1.1 [37]) has been approximately chosen. A curve over the tooth surface was developed in

Unigraphics®, such that the length of the arc is nearly equal to the face width of the mating gear. It is assumed that the force components act on a single face of the tooth at any given point in time. Elements with common faces exist at the edge of the tooth and hence the elements that form this edge have not been considered as the area where the forces act. Hence, the criterion for selecting the area for applying the pressure was the actual area of contact, and not the face width or the working depth.

Current Model F Wiper Nominal Dimensions and Center Distance at 23 Degrees C

THE WORM AND GEAR MESH AT THE POINTS ALONG THE LINE OF ACTION. IN OUR WORM-GEAR DESIGN, WE HAVE TWO TEETH IN CONTACT AND TRANSFERRING LOADS AT ANY GIVEN POINT IN THE LINE OF ACTION INTERSECTS AT THE PITCH TIME. DIAMETERS.



ALLOW A CLEARANCE OR BACKLASH AND IS NOT INTENDED TO HAVE TOOTH CONTACT.

Figure 4.1.1 Line of action for worm-worm gear pair [37]

Table 4.1.1 (a) Calculated dimensions of the worm gear

Axial pitch,p _x	L	p _n	Pd	Pc	d _w	а	b	ht
1.92	3.84	1.891	1.662	10.834	6.897	0.602	0.752	1.318
2.4	4.8	2.363	1.329	13.542	8.621	0.752	0.940	1.648
2.88	5.76	2.836	1.108	16.250	10.345	0.903	1.128	1.977
3.072	6.144	3.025	1.039	17.334	11.035	0.963	1.204	2.109
3.168	6.336	3.119	1.007	17.875	11.380	0.993	1.241	2.175
3.264	6.528	3.214	0.977	18.417	11.725	1.023	1.279	2.241
3.36	6.72	3.308	0.950	18.959	12.070	1.053	1.316	2.307
3.456	6.912	3.403	0.923	19.500	12.414	1.083	1.354	2.373
3.552	7.104	3.497	0.898	20.042	12.759	1.113	1.392	2.439
3.648	7.296	3.592	0.875	20.584	13.104	1.143	1.429	2.505
3.744	7.488	3.687	0.852	21.125	13.449	1.173	1.467	2.571
3.84	7.68	3.781	0.831	21.667	13.794	1.204	1.504	2.637
4.32	8.64	4.254	0.739	24.376	15.518	1.354	1.692	2.966
4.8	9.6	4.726	0.665	27.084	17.242	1.504	1.881	3.296
5.28	10.56	5.199	0.604	29.792	18.966	1.655	2.069	3.625
5.76	11.52	5.672	0.554	32.501	20.691	1.805	2.257	3.955
6.24	12.48	6.144	0.511	35.209	22.415	1.956	2.445	4.284
6.72	13.44	6.617	0.475	37.917	24.139	2.106	2.633	4.614
7.2	14.4	7.090	0.443	40.626	25.863	2.257	2.821	4.944
7.68	15.36	7.562	0.415	43.334	27.587	2.407	3.009	5.273
8.16	16.32	8.035	0.391	46.043	29.312	2.558	3.197	5.603
8.64	17.28	8.507	0.369	48.751	31.036	2.708	3.385	5.932
9.12	18.24	8.980	0.350	51.459	32.760	2.858	3.573	6.262
9.6	19.2	9.453	0.332	54.168	34.484	3.009	3.761	6.591

Table 4.1.1 (b) Calculated dimensions of the worm gear (cont.)

Axial pitch,px	d _o	d _i	Fg	tw	height	pitch dia of gear	h _k ,working depth	Area of contact
1.92	8.100	5.464	4.621	0.94	1.318	61.11	1.20	5.56
2.4	10.12	6.830	5.776	1.18	1.648	76.39	1.50	8.69
2.88	12.15	8.196	6.931	1.41	1.977	91.67	1.81	12.51
3.072	12.96	8.742	7.393	1.51	2.109	97.78	1.93	14.24
3.168	13.36	9.015	7.624	1.56	2.175	100.8	1.99	15.14
3.264	13.77	9.289	7.856	1.60	2.241	103.9	2.05	16.07
3.36	14.17	9.562	8.087	1.65	2.307	106.9	2.11	17.03
3.456	14.58	9.835	8.318	1.70	2.373	110.0	2.17	18.02
3.552	14.98	10.10	8.549	1.74	2.439	113.0	2.23	19.03
3.648	15.39	10.38	8.780	1.79	2.505	116.1	2.29	20.08
3.744	15.79	10.65	9.011	1.84	2.571	119.1	2.35	21.15
3.84	16.20	10.92	9.242	1.89	2.637	122.2	2.41	22.25
4.32	18.22	12.29	10.39	2.12	2.966	137.5	2.71	28.15
4.8	20.25	13.66	11.55	2.36	3.296	152.7	3.01	34.76
5.28	22.27	15.02	12.70	2.59	3.625	168.0	3.31	42.06
5.76	24.30	16.39	13.86	2.83	3.955	183.3	3.61	50.05
6.24	26.32	17.75	15.01	3.07	4.284	198.6	3.91	58.74
6.72	28.35	19.12	16.17	3.30	4.614	213.9	4.21	68.13
7.2	30.37	20.49	17.32	3.54	4.944	229.1	4.51	78.21
7.68	32.40	21.85	18.48	3.78	5.273	244.4	4.81	88.98
8.16	34.42	23.22	19.63	4.01	5.603	259.7	5.11	100.4
8.64	36.45	24.58	20.79	4.25	5.932	275.0	5.42	112.6
9.12	38.47	25.95	21.94	4.49	6.262	290.3	5.72	125.4
9.6	40.50	27.31	23.104	4.726	6.591	305.58	6.02	139.03

Table 4.1.2 (a) Forces acting on the worm tooth

p _x	Torque,T _g (N-m)	Torque,T _w (N-m)	F _x '(N)	F _y '(N)	F _z '(N)
1.92	34	0.8643	-250.635	-1112.64	292.2343
2.4	34	0.8643	-200.508	-890.117	233.7874
2.88	34	0.8643	-167.090	-741.764	194.8228
3.072	34	0.8643	-156.647	-695.404	182.6464
3.168	34	0.8643	-151.900	-674.331	177.1117
3.264	34	0.8643	-147.432	-654.498	171.9025
3.36	34	0.8643	-143.220	-635.798	166.9910
3.456	34	0.8643	-139.242	-618.137	162.3524
3.552	34	0.8643	-135.478	-601.431	157.9645
3.648	34	0.8643	-131.913	-585.603	153.8075
3.744	34	0.8643	-128.531	-570.588	149.8637
3.84	34	0.8643	-125.317	-556.323	146.1171
4.32	34	0.8643	-111.393	-494.510	129.8819
4.8	34	0.8643	-100.254	-445.059	116.8937
5.28	34	0.8643	-91.1402	-404.599	106.2670
5.76	34	0.8643	-83.5452	-370.882	97.4114
6.24	34	0.8643	-77.1187	-342.353	89.9182
6.72	34	0.8643	-71.6102	-317.899	83.4955
7.2	34	0.8643	-66.8362	-296.706	77.9291
7.68	34	0.8643	-62.6589	-278.161	73.0586
8.16	34	0.8643	-58.9731	-261.799	68.7610
8.64	34	0.8643	-55.6968	-247.255	64.9409
8.832	34	0.8643	-54.4860	-241.879	63.5291
9.12	34	0.8643	-52.7654	-234.241	61.5230
9.6	34	0.8643	-50.1271	-222.529	58.4469

Table 4.1.2 (b) Forces acting on the worm tooth (cont.)

		load per too	th		DLOAD	
p _x	F _x (N)	F _y (N)	F _z (N)	P _x	Py	Pz
1.92	-125.317	-556.323	146.1171	-22.5338	-100.034	26.2738
2.4	-100.254	-445.059	116.8937	-11.5373	-51.2175	13.4522
2.88	-83.5452	-370.882	97.4114	-6.6767	-29.6398	7.7848
3.072	-78.3236	-347.702	91.3232	-5.5014	-24.4224	6.4145
3.168	-75.9502	-337.165	88.5558	-5.0163	-22.2688	5.8489
3.264	-73.7164	-327.249	85.9513	-4.5866	-20.3611	5.3478
3.36	-71.6102	-317.899	83.4955	-4.2046	-18.6653	4.9024
3.456	-69.6210	-309.068	81.1762	-3.8638	-17.1527	4.5051
3.552	-67.7394	-300.715	78.9822	-3.5589	-15.7991	4.1496
3.648	-65.9567	-292.801	76.9038	-3.2853	-14.5844	3.8306
3.744	-64.2656	-285.294	74.9319	-3.0390	-13.4910	3.5434
3.84	-62.6589	-278.161	73.0586	-2.8167	-12.5043	3.2842
4.32	-55.6968	-247.255	64.9409	-1.9783	-8.7822	2.3066
4.8	-50.1271	-222.529	58.4469	-1.4422	-6.4022	1.6815
5.28	-45.5701	-202.299	53.1335	-1.0835	-4.8101	1.2634
5.76	-41.7726	-185.441	48.7057	-0.8346	-3.7050	0.9731
6.24	-38.5593	-171.176	44.9591	-0.6564	-2.9141	0.7654
6.72	-35.8051	-158.949	41.7478	-0.5256	-2.3332	0.6128
7.2	-33.4181	-148.353	38.9646	-0.4273	-1.8969	0.4982
7.68	-31.3295	-139.080	36.5293	-0.3521	-1.5630	0.4105
8.16	-29.4865	-130.899	34.3805	-0.2935	-1.3031	0.3423
8.64	-27.8484	-123.627	32.4705	-0.2473	-1.0978	0.2883
8.832	-0.02724	-0.12094	0.031765	-0.00023	-0.00102	0.00027
9.12	-26.3827	-117.120	30.7615	-0.2103	-0.9334	0.2452
9.6	-25.0636	-111.264	29.2234	-0.1803	-0.8003	0.2102

4.2. MODEL DEFINITION

A static analysis was performed on the simplified model of the worm. The worm is "encastred" on both ends of the shaft. Initially a 2-d mesh (Tria3) was developed on the surface of the model, which was then developed into a 3d (C3D4 elements). Number of the nodes and elements used for different models are in Table 4.2.1.

Table 4.2.1. No. of nodes and elements used in the FEA analysis

axial pitch,p _x (mm)	p _x /1.92	no. of nodes	no. of elements
1.92	1	3132	12645
2.4	1.25	3654	15150
2.88	1.5	18276	93270
3.072	1.6	8174	35109
3.36	1.75	6911	29571
3.84	2	6780	28949
4.32	2.25	9269	40478
4.8	2.5	6780	28949
5.28	2.75	11758	51793
5.76	3	9030	39528
6.24	3.25	13440	59655
6.72	3.5	12436	55879
7.2	3.75	13418	59062
7.68	4	10461	46230
8.16	4.25	9128	40152
8.64	4.5	9956	44270
8.832	4.6	13846	61319
9.12	4.75	13484	59376
9.6	5	10141	44684

Material properties (Table 4.2.2) and boundary conditions were assigned to the model in Hypermesh® and solved using ABAQUS solver. Material

properties for unfilled polymer and glass reinforced composite at initial time, t₀, were available from experiments while the common properties published for AISI 1144 steel were considered. [43]. Material properties at the end of 5 years and 10 years were obtained as discussed in Chapter 3.1.3.

Table 4.2.2. Assumed material properties at initial time, to

GC25A	· · · · · · · · · · · · · · · · · · ·		
Temperature (Celsius)	Е, Мра	sigma u, Mpa	sigma y, Mpa
-40	10257.372	138.34	20.514
23	8816.213	94.926	17.632
105	4854.369	47.145	9.708
M90			
	E, Mpa	sigma u, Mpa	sigma y, Mpa
-40	3588.220	83.001	7.176
			
23	2857.670	54.387	5.715
105	952.780	20.925	1.905
Steel	E Mas	eigma u	sigma y, Mpa
Steel	E, Mpa 	sigma u, Mpa	
23	210000	584.7	346.8

Elasto-plastic analysis was performed on the model where material properties were known from experiments, whereas, elastic analysis was performed for the extrapolated values. In both cases, the size of the model was increased until the maximum stress was either less than or equal to the yield stress of the material. The results obtained (Table 4.2.3 (a), (b), (c), 4.2.4 (a), (b), (c), 4.2.5were based on two criteria: 1) yield stress is 0.2% of the tensile strength (from experiments conducted at MSU) of the material 2)

safe stress published elsewhere. [7]. The elasto-plastic analysis of the model is defined in the input file as follows (the number of nodes and elements have been reduced as they occupy great amount of space):

```
** ABAQUS Input Deck Generated by HyperMesh Version: 5.1
** Generated using HyperMesh-Abaqus Template Version: 5.1-1
   Template: ABAQUS/STANDARD 3D
*NODE
     1, 1.497510028E-14, 35.0
                                   . 4.2325
                       , 33.99344002519 . 4.2325
     2. 0.0
     3. 0.0
                       , 32.986880050381, 4.2325
     4. 0.0
                       , 31.980320075572, 4.2325
     5, 0.0
                       , 30.973760100763, 4.2325
     6. 0.0
                       , 29.967200125954, 4.2325
*ELEMENT,TYPE=C3D4,ELSET=n1
   4164.
           2491,
                    1921.
                             2063.
                                     1910
            2001,
   4165,
                    1877,
                             1878,
                                     1921
   4166,
           2368,
                    916,
                            929,
                                    2392
   4167.
            1223,
                    1781,
                            2229.
                                     2131
   4168.
           2510,
                     750,
                            2455.
                                    2511
   4169.
           2673.
                    1563.
                             1582.
                                     1740
            1584.
   4170.
                     73.
                           1752.
                                     72
*SOLID SECTION, ELSET=n1, MATERIAL=GC25A
**HMCOLOR COMP
                        6
                          10
*NSET, NSET=nset1
   53.
         54.
                                              60,
                55.
                      56,
                            57,
                                  58,
                                        59.
   61.
        1531,
               1532.
                       1533.
                                     1535,
                                             1536,
                              1534.
                                                    1537,
                              1561, 1562,
  1538,
         1558, 1559, 1560,
                                              1578.
                                                    1579.
  1588.
*ELSET, ELSET=elem1
  4278.
         4362,
                4397,
                        4578,
                               4616,
                                      4901,
                                              5087,
                                                     5107.
         5396,
  5118,
                5401,
                        5677,
                               5887,
                                      5889.
                                              5934.
                                                     5995.
  5996,
         6159,
                6160,
                        6169.
                               6208.
                                      6496.
                                              6498,
                                                     6537,
  6596,
         6770.
                6860,
                        8098,
                               8225,
                                      9076
*MATERIAL, NAME=GC25A
*DENSITY
1.5800E-09,23.0
*ELASTIC, TYPE = ISOTROPIC
8816.21 ,0.47
                 .23.0
*PLASTIC, HARDENING=ISOTROPIC
17.63
        .0.0
                ,23.0
20.679
        ,0.000654 ,23.0
23.156 ,0.00137
                  ,23.0
27.158
        ,0.00292
                  ,23.0
30.410
       ,0.00455
                  ,23.0
```

```
33.199
         .0.00623
                   ,23.0
 38.936
         ,0.01058
                   .23.0
 43.599
         .0.01505
                   ,23.0
 47.596
         ,0.0196
                  ,23.0
 51.133
         .0.0242
                  ,23.0
 54.328
         ,0.0288
                  ,23.0
 57.257
         .0.0335
                  ,23.0
 59.971
         ,0.0382
                  .23.0
62.507
         .0.0429
                  ,23.0
64.894
         ,0.0476
                  .23.0
67.152
         ,0.0524
                  .23.0
69.299
         .0.0571
                  .23.0
71.348
        .0.0619
                  .23.0
73.309
         .0.0667
                  ,23.0
75.193
         ,0.0715
                  .23.0
82.088 ,0.0907
                  .23.0
*STEP. INC = 1000, NLGEOM
**HMNAME LOADCOL
                          4 loadcol
**HMCOLOR LOADCOL
                            4 15
*STATIC
0.1
       ,1.0
*BOUNDARY
    1963, ENCASTRE
    1962.ENCASTRE
    1961, ENCASTRE
    1960, ENCASTRE
    1959, ENCASTRE
    1958.ENCASTRE
    1957, ENCASTRE
    1956, ENCASTRE
    1955, ENCASTRE
*DLOAD, OP=MOD
   9076, P3,26.27
   6169, P3,26.27
   5401, P3,26.27
   6208, P1,26.27
   9076, P3,-100.03
   6169, P3,-100.03
   5401, P3,-100.03
   6208, P1,-100.03
   9076, P3,-22.53
   6169, P3,-22.53
   5401, P3,-22.53
   6208, P1,-22.53
*NODE FILE
U,
RF.
*EL FILE
S,
```

```
SP,
SINV,
E,
EP,
PE,
*NODE PRINT,FREQUENCY= 2
U,
*EL PRINT,FREQUENCY= 2
S,
SP,
MISES,
E,
SINV,
EP,
PE,
*END STEP
```

FEA ANALYSIS RESULTS

yield stress from current work— $\triangleright \sigma_{y1}$ yield stress from Clifford E. Adams [7]— $\triangleright \sigma_{y2}$

ELASTO-PLASTIC ANALYSIS

Table 4.2.3 (a) FEA results for GC25A at 23C at to

GC25A@23C	$\sigma_{y1} = 17.63$ Mpa	σ _{y2} = 48.26 Mpa			
axial pitch, p _x (mm)	axial pitch increased by	Von Mises stress,Mp a	Displacemen t (mm)	Equivalen t plastic strain	
1.92	0%	82.090	3.0330	1.7600	
2.88	50%	48.700	0.0675	0.0210	
3.072	60%	31.980	0.030	0.005	
3.84	100%	22.8600	0.0194	0.0013	
4.32	125%	17.6600	0.0126	0.0000	7.131E- 06
4.8	150%	10.9200	0.0090	0.0000	

ELASTIC ANALYSIS (TTS) [after 5yrs]

Table 4.2.3 (b) FEA results for GC25A at 23C after 5yrs

TTSGC25A@23C	$\sigma_{y1} = 8.608 \text{ Mpa}$	$\sigma_{y2} = 23.6 \text{ Mpa}$	
axial pitch, p _x (mm)	axial pitch increased by	Von Mises stress,Mpa	Displacement (mm)
3.36	75%	39.2500	0.0438
3.84	100%	29.3400	0.0375
4.32	125%	17.7200	0.0257
4.8	150%	15.0300	0.0192
5.76	200%	10.460	0.01975
6.72	250%	5.315	0.01168

ELASTIC ANALYSIS (TTS) [after 10yrs]

Table 4.2.3 (c) FEA results for GC25A at 23C after 10yrs

TTSGC25A@23C	σ _{y1} = 8.246 Mpa	σ _{γ2} = 22.6 Mpa	
axial pitch, p _x (mm)	axial pitch increased by	Von Mises stress, Mpa	Displacement (mm)
3.84	100%	29.3400	0.0392
2.4	125%	17.7200	0.0269
5.76	200%	10.460	0.02062
6.72	250%	5.315	0.01219

ELASTO-PLASTIC ANALYSIS

Table 4.2.4 (a) FEA results for GC25A at 105C at to

GC25A@105C	$\sigma_{y1} = 9.71 \text{ Mpa}$	σ _{y2} = 26.57 Mpa		
axial pitch, p _x (mm)	axial pitch increased by	Von Mises stress,Mpa	Displacemen t (mm)	Equivalent plastic strain
1.92	0%	•	-	-
2.88	50%	33.080	0.149	0.047
3.072	60%	24.680	0.065	0.020
3.36	75%	21.530	0.052	0.013
3.84	100%	17.810	0.041	0.007
4.32	125%	11.780	0.019	0.00096
4.8	150%	9.485	0.013	0.000

ELASTIC ANALYSIS (TTS) [after 1yr]

Table 4.2.4 (b) FEA results for GC25A at 105C after 5yrs

TTSGC25A@105C	$\sigma_{y1} = 2.246 \text{ Mpa}$	$\sigma_{y2} = 6.15 \text{ Mpa}$	
axial pitch, p _x (mm)	axial pitch increased by	Von Mises stress,Mpa	Displacement (mm)
3.84	100%	25.3700	0.1178
5.76	200%	9.0210	0.0633
6.24	225%	5.2600	0.0412
6.72	250%	4.7860	0.0371
7.2	275%	3.7400	0.0338
8.16	325%	2.2020	0.0209
8.64	350%	1.8370	0.0191
9.6	400%	1.5120	0.0159

ELASTIC ANALYSIS (TTS) [after 10yrs]

Table 4.2.4 (c) FEA results for GC25A at 105C after 10yrs

TTSGC25A@105C	$\sigma_{y1} = 1.78 \text{ Mpa}$	$\sigma_{y2} = 4.88 \text{ Mpa}$	
axial pitch, p _x (mm)	axial pitch increased by	Von Mises stress,Mpa	Displacement (mm)
6.24	225%	5.259	5.2590
6.72	250%	4.787	0.0467
7.2	275%	3.74	0.0426
7.68	300%	3.117	0.0316
8.832	360%	1.936	0.0265
9.12	375%	1.888	0.0255
9.6	400%	1.512	0.0201

ELASTO-PLASTIC ANALYSIS

Table 4.2.5. FEA results for GC25A at -40°C at to

GC25A@ 40C	$\sigma_{y1} = 20.51 \text{ Mpa}$	$\sigma_{y2} = 56.14 \text{ Mpa}$		
axial pitch, p _x (mm)	axial pitch increased by	Von Mises stress,Mpa	Displacem ent (mm)	Equivalent plastic strain
1.92	0%	134.400	1.192	0.543
2.88	50%	58.760	0.059	0.017
3.84	100%	26.470	0.020	0.00103

ELASTO-PLASTIC ANALYSIS

Table 4.2.6. FEA results for AISI 1144 Steel

Steel	$\sigma_{y1} = 346.8 \text{ Mpa}$	[Ref: efunda.com]		
axial pitch, p _x (mm)	Von Mises stress,Mpa	Displacement (mm)	Equivalent plastic strain	
1.92	348.500	0.008	0.000	9.21E-05

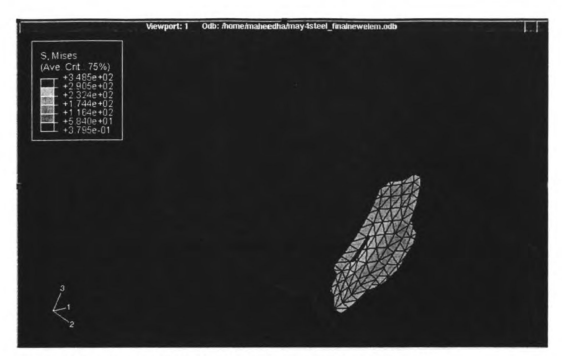


Figure 4.2.1. σ_{max} for Steel (axial pitch=1.92mm)—Left View

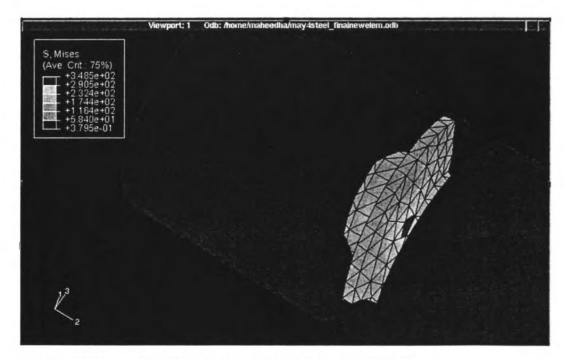


Figure 4.2.2 σ_{max} for Steel (axial pitch=1.92mm)—Right View



Figure 4.2.3. Equivalent plastic strain for Steel (axial pitch=1.92mm)

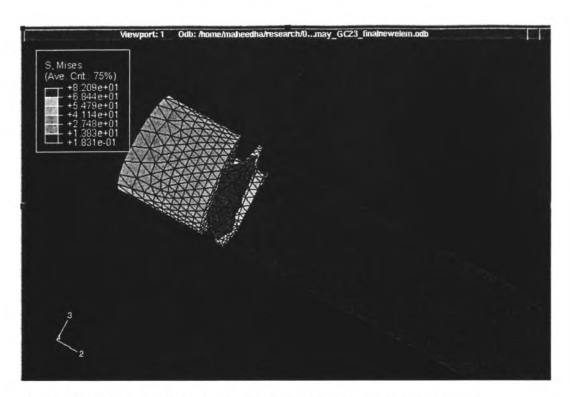


Figure 4.2.4. σ_{max} for GC25A@23C at time, t_0 (axial pitch=1.92mm)

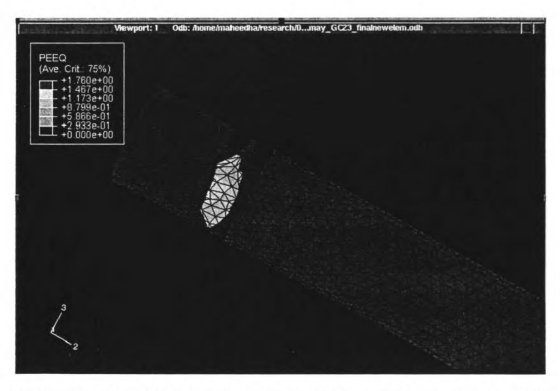


Figure 4.2.5.Equivalent plastic strain for GC25A@23C at time, t_0 (axial pitch=1.92mm)

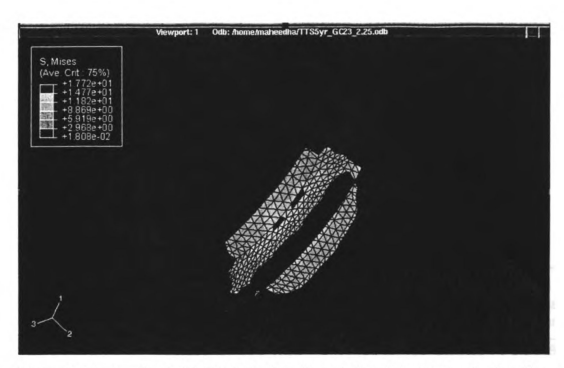


Figure 4.2.6. σ_{max} for GC25A@23C after 10yrs (axial pitch=2.25mm)—Left View

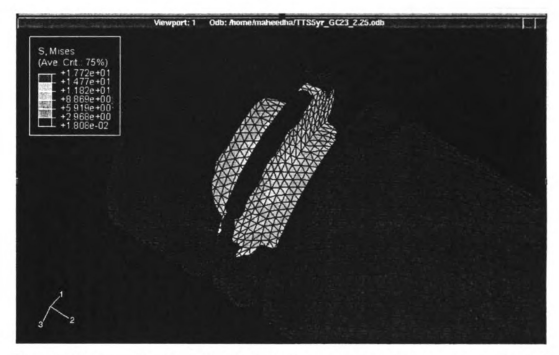


Figure 4.2.7. σ_{max} for GC25A@23C after 10yrs(axial pitch=2.25mm)—Right View

4.3. COST ANALYSIS

The lead required for lifting the window through some distance is constant; hence the same travel is required for the redesigned composite gear. The volume of the composite required (based on calculations shown in Chapter 3.4) would be as in Table 4.3.1.

Table 4.3.1 Volume of composite material required

axial pitch (mm)	% increase in axial pitch	Volume of helical thread (mm3)	Volume of solid shaft (mm3)	Total Volume (mm ³)	Mass of GC25A (Kg)	Price of acetal (dollars)
1.920	0%	1028.290	3557.853	4586.144	0.0072	0.014813
2.880	50%	2314.437	9559.431	11873.868	0.01876	0.038353
3.072	60%	2633.105	10876.508	13509.614	0.02134	0.043636
3.840	100%	4116.813	16994.545	21111.358	0.03335	0.06819
4.320	125%	5208.666	21508.721	26717.387	0.04221	0.086297
6.240	225%	10867.805	44876.220	55744.025	0.08807	0.180053
6.720	250%	12603.010	52045.794	64648.804	0.10214	0.208816
7.200	275%	14468.971	59746.447	74215.418	0.11726	0.239716
8.160	325%	18583.525	76740.992	95324.518	0.15061	0.307898
9.600	400%	25722.616	106215.906	131938.521	0.20846	0.426161

Chapter 5

SUMMARY AND CONCLUSIONS

Based on the FEA analysis, the mass and cost estimate show that switching to a composite (e.g., GC25A) would reduce weight as well as the material cost. Besides, the machining cost for a steel part is considerably high compared to plastic one. The cost of the machined blank would cost about \$0.20/part while the machining processes such as hobbing, deburring would result in a cost of \$10/part. The plastic part would require less machining (if necessary) and hence the material cost as well as machining cost is much less compared to the steel part. Injection molding (which is generally done in huge quantities, (250,000-500,000 parts) would cost \$0.20/part and the investment cost would be about \$16K-\$20K. These estimates would defer among different manufacturers, but would still result in cheaper processing of plastic parts compared to steel ones [44].

This project did not consider thermo-mechanical issues. Hence, work regarding the thermal aspect should be considered. Future work could be developed by assuming the composite as orthotropic and determining, experimentally, the mechanical properties in different directions. Dynamic modeling and contact analysis could be performed and based on the results obtained; prototype testing of a worm could be conducted.

BIBLIOGRAPHY

- [1] http://science.howstuffworks.com/gear5.htm
- [2] European Plastics news, 1994, Appliance applications, Vol.21, No. 9, p 39
- [3] Ticona
- [4] Walton D, Hooke C. J, Mao K, Breeds A and Kukureka S, 1992, *A New Look at Testing and Rating Non-metallic Gears*, 3rd Edition, World Congress on Gearing and Power Transmission
- [5] Dupont Engineering Polymers Catalog, p 9
- [6] Bosch, 2000, Automotive Handbook, 2nd Edition, p 772
- [7] Clifford E. Adams, 1986, *Plastics Gearing*, Selection and Application, p 156
- [8] Tascher Gerhard, Pfendler Klaus, 2002, *Electro-motor Drive in automatic door using worm gear*, European Patent Application No.: EP1235330A1
- [9] Hooke C. J, Mao. K, Walton D, Breeds A. R. and Kukureka S. N, 1993, Measurement and Prediction of the Surface Temperature in Polymer Gears and Its Relationship to Gear Wear, Journal of Tribology, Vol.115, p119
- [10] Walton D, Cropper A. B, Weale D. J, and Klein Meuleman P, 2002, *The efficiency and friction of plastic cylindrical gears, Part 1: Influence of materials*, Proc Instn. Mech. Engrs, Vol. 216, Part J, J Engineering Tribology
- [11] Ding, Jianning, 1993, Experimental Study of The Composite Material based on Polymer Worm Gear Transmission Lubricated under O/W Emulsions, Lubrication Engineering, Vol. 4, p. 18

- [12] Walton D, Hooke C. J, Mao K, 1991, New aspects of performance for non-metallic gears, European Engineering Research and Tech. Transfer Congress, Vol. 1-3, Issue: paper 412/149
- [13] Vilmos Simon, 1996, Stress Analysis in Worm Gears with Ground Concave Worm Profile
- [14] Henri Yelle and R.Gauvin, 1980, *Plastic gears put teeth into old designs*, Canadian Plastics, Vol.38, No. 4
- [15] John W. Kelley, 1998, *Materials selection and design for gears in stalled conditions*, Proc. Of 1998 56th Annual Tech. Conference, ANTEC, Part 3,Vol.3
- [16] Paul Wyluda and Dan Wolf, Examination of finite element analysis and experimental results of quasi-statically loaded acetal copolymer gears, 2002, Annual Tech. Conference, ANTEC
- [17] Kenichi Terashima, Naohisa Tsukamoto and Jiasun Shi, 1984, Development of Plastic Gears for Power Transmission, Bulletin of JSME, Vol.27, No. 231
- [18] Naohisa Tsukamoto, 1981, Investigation about the Strength of Plastic Gear (2nd report; Abrasion of the Nylon Gear for Power Transmission, Meshing with the Steel Gear), Bulletin of the JSME, Vol.24, No. 191
- [19] Crippa G. and Davoli P., 1995, Comparative Fatigue Resistance of Fiber Reinforced Nylon 6 Gears, Journal of Mechanical Design, Vol.117, p193
- [20] Wolf L. J, Diboll W. B. (Jr), 1965, *The Role of Stress Concentration in the Fatigue of Delrin*, Journal of Engineering for Industry, p 319-322
- [21] Woodley B. J, Michael Neale and Assoc. Ltd, 1977, *Materials for Gears*, Tribology International, p 323-331
- [22] Lawrence E. Nielson and Robert F. Landel, 1994, *Mechanical Properties of Polymers and Composites*, 2nd Edition, p 342

- [23] Ming-Haung Tsai, Ying-Chein Tsai, 1997, *A Method for calculating static transmission errors of plastic spur gears using FEM evaluation*, Finite Elements in Analysis and Design, Vol. 27, p 345-357
- [24] Kenichi Terashima, Naohisa Tsukamoto, Noriteru Nishida, 1986, Development of Plastic Gears for Power Transmission (Design on Load-carrying Capacity), Bulletin of JSME, Vol.29, No. 250, p 1326-1329
- [25] Yelle H, 1981, Root Bending Fatigue Strength of Acetal Spur Gears A Design Approach to Allow for Load Sharing, AGMA Fall Tech. Meeting, Toronto, Canada, Paper P149.01
- [26] Naohisa Tsukamoto, 1979, Investigation about the Strength of Plastic Gears, Bulletin of the JSME, Vol. 22, No. 173, p 1685-1692
- [27] Hooke C. J, Kukureka S. N, Liao P, Rao M, Chen Y. K, 1996, *The friction and wear of polymers in non-conformal contacts*, Wear, Vol. 200, p 83-94
- [28] Kenichi Terashima, Naohisa Tsukamoto, Noriteru Nishida, 1986, Development of Plastic Gears for Power Transmission (Economical Methods for Increasing Load-carrying Capacity), Bulletin of JSME, Vol.29, No. 247, p 256-259
- [29] http://www.psrc.usm.edu/macrog/mech.htm
- [30] Onoki S, *Mechanical Properties of Polymers and Composites*, 1982, p215, Kagakudoninsha
- [31] Nader E. Abedrabbo, 2002, Experimental and Numerical Investigations of Stamp Hydroforming and Ironing of Wrinkling in Sheet Metal Forming, Master of Science Thesis, Michigan State University
- [32] J. L. Sullivan, Y. F. Wen and R. F. Gibson, 1993, Fundamental Aspects of Composite Viscoelastic Behavior, Materials and Mechanics Issues, ASME 1993, MD-Vol. 46, p195-196
- [33] TA Instruments, Application of Time-Temperature Superposition Principle to DMA, Thermal Analysis Application Brief, Number TA-144

- [34] TA Instruments Rheology Advantage Data Analysis online Help Manual
- [35] Sujan E. Bin Wadud, *Time-Temperature Superposition Using DMA Creep Data*, TA-287
- [36] William P. Crosher, Design and Application of the Worm Gear, 2002, p 35
- [37] Visteon Wiper/Washer Engineering
- [38] Norton, L., Machine Design, An Integrated Approach, 2000 p. 780
- [39] Robert C. Juvinall, Kurt M. Marshek, 1999, Fundamentals of Machine Component Design, p. 707
- [40] http://newton.dep.anl.gov/askasci/math99/math99080.htm
- [41] ABAQUS, INC., 1080 Main Street, Pawtucket, Rhode Island, 02860-4847, USA.
- [42] http://islnotes.cps.msu.edu/trp/inj/int_bas.html#material
- [43] http://www.efunda.com/materials/alloys/alloy_home/steels_properties.cfm
- [44] Representative from ITW Spiroid, Chicago, IL

